



INSTITUTO DE
TECNOLOGÍA
QUÍMICA



EXCELENCIA
SEVERO
OCHOA



CSIC
CONSEJO SUPERIOR DE INVESTIGACIONES CIENTÍFICAS



UNIVERSITAT
POLITÈCNICA
DE VALÈNCIA

Thin Film Proton and Mixed Conductors

Trabajo Final de máster en Química Sostenible

Por:

Colin Hannahan

Directors:

José Manuel Serra Alfaro

Fidel Toldra Reig

September 2019



INSTITUTO DE
TECNOLOGÍA
QUÍMICA



EXCELENCIA
SEVERO
OCHOA

2



CSIC
CONSEJO SUPERIOR DE INVESTIGACIONES CIENTÍFICAS



UNIVERSITAT
POLITÈCNICA
DE VALÈNCIA

Table of Contents

1. Introduction.....	4
1.1. Thin Film Supported Membranes	4
1.2. Process Intensification.....	7
1.3. Proton Conducting Membranes.....	7
1.4. Proton Conduction Mechanisms.....	10
1.5. Mixed Ion Conducting Membranes.....	12
1.6. Defect Theory	13
2. Objectives.....	14
3. Experimental Methodology	15
3.1. Material Synthesis	15
3.1.1. Co-precipitation	15
3.2. Material Selection	15
3.2.1. Gadolinium Doped Cerium Oxide (CGO).....	15
3.2.2. Palladium and Alloys.....	16
3.2.3. Calcium Doped Gadolinium Oxide (GCO)	18
3.2.4. Substrates	19
3.2.5. BCZYYb	19
3.2.6. Commercial Ceramic Membranes – Anodisc/A-tech	20
3.3. Sputtering.....	21
3.4. Characterization Methods	22
3.4.1. X-ray Diffraction	22
3.4.2. Scanning electron microscopy	23
3.4.3. Energy Dispersive X-ray Spectroscopy.....	24
3.4.4. Electrochemical Characterization	24
4. Discussion of Results	26
4.1. Palladium membranes.....	26
4.2. GCO	32
4.3. GCO on Palladium.....	34
4.4. CGO on BCZYYb.....	36
5. Future Action	43
6. Conclusions.....	44
7. Bibliography	47
Agradecimientos:	50



1. Introduction

In its most simple and perfect form a membrane can be thought of as a molecular scale filter. An ideal membrane will take a mixture of two compounds, A and B, and produce a pure permeate of compound A and a non-permeating compound B. Given the intense research in the field of membrane separation over the past 30 years, some membranes have approached the simplicity and separation capacity of these ideal devices. Usually, membrane-based separations require more complex operation schemes. For example, If the two compounds are not separated perfectly in a single pass, recycling steps will be required. Often the feed streams must undergo expensive, energy intensive compression steps in order to provide the pressure difference which drives many membrane-based separations. Nonetheless, steady progress in the field has caused for the removal of some of these limitations. Membranes now exist in a territory once occupied by traditional separation techniques such as absorption and cryogenic distillation. Some advantages which membranes hold over traditional methods are low energy consumption, continuous separation, mild process conditions, scalability and compatibility with other separation techniques. Considering these advantages, it is easy to forget that there is much work left to be done so that gas separation membranes can meet their potential. Recognizing the current limitations of membranes is key to their improvement. One such limitation is their inadequate production capacity. A way in which this issue is being addressed is by reducing membrane thickness down to the nanoscale. However, upon this reduction in thickness, new problems arise such as pinhole defects and cracks in the membrane. These mechanical issues compromise the all-important selectivity and durability of the membrane. This work will focus on certain classes of these reduced thickness membranes often referred to as thin films. The general goal of this project is to better understand how deposition conditions and post processing techniques affect the physical nature of thin films comprised of various materials. Information such as this is crucial in the development of effective and dependable gas separation membranes.

1.1. Thin Film Supported Membranes

Two major hurdles along the way to commercializing membranes are cost and production capacity. Constructing a bulk membrane from a noble metal such as palladium is expensive and impractical. One way to overcome this is to employ ultra-thin membranes which require far less material and initial investment than their bulk counterparts. An additional advantage is the increased flux of gases through the thin films. Flux is a key parameter to consider for gas separation and is defined as the number



INSTITUTO DE
TECNOLOGÍA
QUÍMICA



EXCELENCIA
SEVERO
OCHOA

4



CSIC
CONSEJO SUPERIOR DE INVESTIGACIONES CIENTÍFICAS



UNIVERSITAT
POLITÈCNICA
DE VALÈNCIA

of moles of gas diffusing through a perpendicular unit of cross-sectional area per unit time. Low flux is a disadvantage for many types of bulk membranes and increasing it would be a key step to implementing membranes industrially.

The derivation for the steady state flux of gases through a non-porous membrane begins with Fick's first law shown in equation 1. D is the diffusion coefficient, which is multiplied by the concentration gradient across the membrane. Since surface concentration is not a measurable quantity, Henry's law must be applied. In equation 2, a method for calculating flux using only measurable quantities is presented. In this equation, Φ is the permeability term which is simply the product of diffusivity and solubility of the gas in the membrane. The value of n changes depending on the prevailing transport mechanism. For very thin membranes n will approach 1. This is because the diffusion rate is proportional to the gas pressure. In this equation, it is obvious how thin film membranes provide higher fluxes as x is the variable which represents membrane thickness. It should also be noted that permeability is a material constant independent of membrane thickness but that it does have an Arrhenius type relationship with temperature [1] [2].

$$J = -D \frac{\partial C}{\partial x}$$

Equation 1: Fick's Law of Diffusion

$$J = \frac{\Phi (p_1^n - p_2^n)}{x}$$

Equation 2: Fick's law of diffusion with measurable variables [2]

The combination of increased flux and lower investment costs make thin film membranes economically attractive. In one study, it was concluded that at a thickness of 0.05 mm palladium membranes require a similar level of investment to conventional techniques such as pressure swing adsorption. At a thickness of 0.01 mm membranes become the most inexpensive technology for hydrogen separation. A graph showing the effect of membrane thickness on specific investment is shown in figure 5 [3].



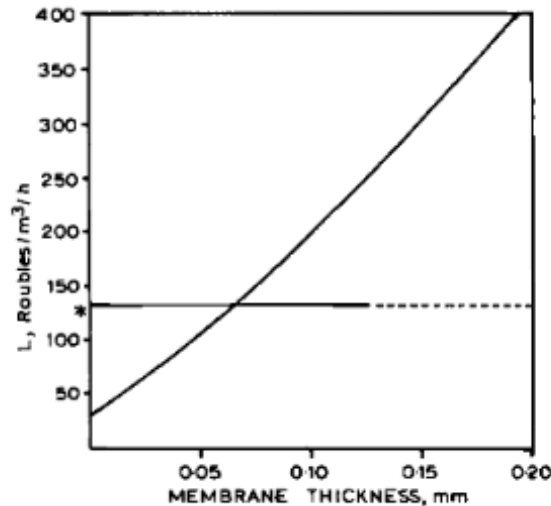


Figure 1: Chart showing relationship between membrane thickness and initial investment. The horizontal line represents the investment level for pressure swing adsorption [3].

Despite the benefits of ultra-thin membranes, they lack sufficient mechanical strength to operate consistently on industrial scales. To overcome this, a more durable porous material is used as a support for the thin film. The three principal types of support materials are glass, ceramic and stainless steel. Each type of support possesses its own advantages and is chosen based on the application for which the membrane will be used. In this work, porous ceramic materials are used as supports for the thin film membranes. Alumina is the most widely used material for ceramic supports because it is available in many different compositions and has high thermal and mechanical stability [1].

There are several different methods available for the deposition of thin films onto porous supports. In general, film deposition techniques fall into two categories. These are physical vapor deposition (PVD) and chemical vapor deposition (CVD). Physical vapor deposition is a process in which a material is removed from a target and deposited onto a substrate. PVD generally allows for refined tuning of film properties and good rate control. It is also useful for the fast deposition of complex ceramic materials. Some examples of PVD methods are sputtering, evaporation and laser ablation. CVD is a material synthesis method in which gaseous compounds undergo reactions at a surface to form a solid film. It is a more difficult method to control due to the complex reactions occurring at the substrate surface. Examples of CVD methods include electroplating and the sol-gel method. In this work, PVD is employed in the form of magnetron sputtering which will be explained in greater detail in a later section [4].

1.2. Process Intensification

In the field of chemical engineering, process intensification (PI) is a topic which has gained significant momentum in recent years. The concept of process intensification is broad and can be applied in many different situations. Stankiewicz and Moulijn defined process intensification in 2000 as the development of novel and sustainable equipment that compared to the existing state-of-the-art, produces dramatic process improvements related to equipment sizes, waste production, and other factors. This definition is simple, but its ramifications are massive as the potential benefits in cost and sustainability are great.

Process intensification can be divided into two areas. These are process intensifying equipment and process intensifying methods. PI equipment are process units which are specialized to optimize critical variables such as heat transfer and mass transfer. A reactive distillation unit is an example of a process intensifying piece of equipment. An intensifying unit such as this combines a chemical reactor and a distillation column into one and leads to 20-80% reduction in capital costs and/or energy usage. A process intensified method integrates multiple process steps into a single unit operation or uses an alternative energy source. An example of a process intensified method would be utilizing microwaves in an assisted reactive distillation unit to enhance a transesterification reaction.

Membranes fit perfectly into the field of PI due to their application in catalytic membrane coupled reactors. A reactor like this is a classic example of a piece of process intensifying equipment as the reaction step is combined with the separation step in one unit. It is like a reactive distillation unit except that the separation step is passive, continuous and more sustainable. Some of these reactors are in use today especially in the wastewater industry. Thin film membranes have the potential to greatly increase the separation capacity and efficiency of these reactors. Currently, thin films lack the durability and stability to maintain their functionality in reactor conditions. This thesis will discuss different types of thin film membranes and seek to further their development towards implementation in process intensifying equipment [5] [6].

1.3. Proton Conducting Membranes

As fossil fuel resources become scarcer and carbon pollution more of an environmental threat, new methods of energy generation must be sought out. Many have coined the 21st century the era of the hydrogen economy due to the element's high energy density



INSTITUTO DE
TECNOLOGÍA
QUÍMICA



EXCELENCIA
SEVERO
OCHOA

7

CONSEJO SUPERIOR DE INVESTIGACIONES CIENTÍFICAS
CSIC



UNIVERSITAT
POLITÈCNICA
DE VALÈNCIA

and carbon free combustion. Whether or not a full hydrogen economy is ever achieved, hydrogen is already a key resource. It is the most abundant gas in the atmosphere with applications in the fuel cell industry, and as a feed stock element in many important industrial processes. At the center of a possible hydrogen revolution is research focused on cheap and sustainable production of high purity hydrogen. Today, steam reforming of methane is the main method used to produce hydrogen. Steam reformation reacts methane with water vapor to create carbon monoxide and hydrogen. The method utilizes the water gas shift reaction to convert CO to hydrogen as well. While steam reformation produces rather high purity hydrogen, most industrial processes require hydrogen with a purity of at least 99.99%. Polymer exchange membrane fuel cells require hydrogen with a purity of 99.9995%. Therefore, separation/purification techniques are necessary to utilize the gas [1].

Currently, the two main methods employed for hydrogen purification are pressure swing adsorption (PSA) and cryogenic distillation. PSA is a method that utilizes a specialized material which adsorbs impurities at high pressure. The impurities are then desorbed at a lower pressure. The operating pressure is cycled between the tail and the feed gas and the impurities are removed from the system. PSA is an attractive option due to its ability to produce ultra-pure hydrogen (99.999%) but there are high energy costs associated with gas compression. Cryogenic distillation takes advantage of the higher boiling point of the impurity gases by separating them via condensation at very low temperatures. This method has the benefit of allowing the collected hydrogen to be stored as a liquid. However, it is a highly energy intensive process that produces relatively low purity hydrogen. Both cryogenic distillation and PSA are particularly difficult to carry out on a small-scale [2].

Due to the energetic disadvantages of PSA and cryogenic distillation, alternative techniques are needed. Membranes are considered a suitable alternative to traditional hydrogen separation methods. Hydrogen selective membranes are advantageous because of their low energy consumption and their ability to perform continuous separation. Proton conductors generally operate using a pressure or concentration gradient as the driving force for gas separation. There are several types of hydrogen selective membranes with different separation mechanisms and physical properties, but they can generally be divided into two principal categories; dense and porous. The gas separation mechanism differs between these two classes. In dense membranes, gas transport usually occurs via solution-diffusion while porous membranes rely on molecular sieving or Knudsen diffusion. This work is focused on two specific types of



INSTITUTO DE
TECNOLOGÍA
QUÍMICA



EXCELENCIA
SEVERO
OCHOA

8



CSIC
CONSEJO SUPERIOR DE INVESTIGACIONES CIENTÍFICAS



UNIVERSITAT
POLITÈCNICA
DE VALÈNCIA

dense proton conducting membranes. They are dense metallic and ceramic membranes composed of palladium and calcium doped gadolinium oxide respectively [4].

Palladium based materials are the most widely studied variation of hydrogen membrane to date. Early work done by Lewis over 50 years ago showed in detail the hydrogen permeation properties of palladium foils. Palladium is widely studied as a membrane due to its innate ability to purify hydrogen to a level greater than 99.9999%. Dense metallic membranes operate at temperatures conducive to many industrial processes and are characterized by a relatively high flux compared to other materials. However, they are subject to poisoning by compounds such as hydrogen sulfide and carbon monoxide. Palladium membranes undergo a phase transition in the presence of reductive conditions at a certain temperature threshold, which can affect the stability and selectivity of the membrane. Researchers address the phase transition issue by alloying with other metals such as copper or silver [1].

Although there has been more research done with metallic membranes, dense ceramic membranes are a viable alternative with similar hydrogen selectivity properties. They operate at a higher temperature than their metallic counterparts which can be advantageous for their use in fuel cells and in electrolysis. Another advantage of ceramic membranes is their chemical inertness. This makes them more resistant to poisoning from gases such as carbon monoxide. A comparison of the properties of the two membrane materials is summarized in Table 1 [4].

	Dense Metallic	Dense Ceramic
Temperature Range (C)	300-600	600-900
Hydrogen Selectivity	> 1000	> 1000
Hydrogen Flux (Units)	60-300	6-80
Stability Issues	Phase Transition	Stability in CO ₂
Poisoning Compounds	H ₂ S, HCl, CO	H ₂ S
Materials	Pd and Pd alloys	Proton Conducting Ceramics
Transport Mechanism	Solution/Diffusion	Solution/Diffusion

Table 1: Comparison of properties of Dense Ceramic and Metallic Membranes [2]



INSTITUTO DE
TECNOLOGÍA
QUÍMICA



EXCELENCIA
SEVERO
OCHOA

9



CSIC
CONSEJO SUPERIOR DE INVESTIGACIONES CIENTÍFICAS



UNIVERSITAT
POLITÈCNICA
DE VALÈNCIA

1.4. Proton Conduction Mechanisms

Hydrogen transport through dense metallic and ceramic membranes occurs via solution-diffusion. In palladium, the following steps are involved in the movement of the gas through the membrane. First, the catalytic properties of the palladium layer allow for the dissociative adsorption of H_2 onto the surface of the membrane. Atomic hydrogen then diffuses through the metal layer and then associatively desorbs as the protons recombine on the permeate side of the membrane [4].

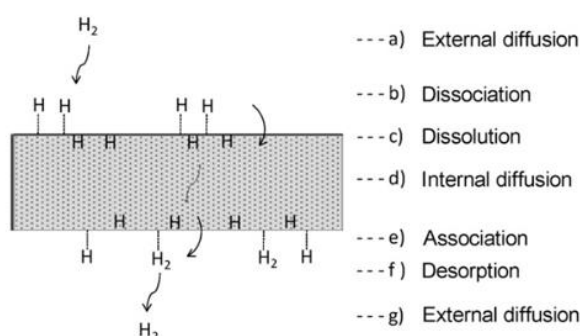


Figure 2: Diagram showing steps of hydrogen diffusing through palladium [1]

The solution stage of solution-diffusion occurs when the hydrogen dissolves in the metal to form a palladium-hydrogen system. The dissolved monoatomic hydrogen occupies interstitial sites within the crystal structure of the metal. Although most transition metals adopt the body centered cubic (BCC) crystal structure, palladium exists as a face centered cubic (FCC) unit cell and maintains this structure upon forming a solution with hydrogen. Both types of unit cells possess octahedral and tetrahedral interstitial sites that are available to be occupied by protons. Diagrams of both cubic unit cells are depicted in figure 3. In the case of palladium, density of states calculations have shown that hydrogen prefers to inhabit the O sites due to their superior stability. Temperature also has a marked effect on hydrogen solubility in metals. Palladium and titanium are known as “exothermic occluders” and exhibit a decrease in hydrogen solubility as temperatures increase. They both have negative enthalpies of hydride formation at their interstitial sites. Practically, this means that hydrogen dissolves easily in the metal and does not require a source of external heat [2].

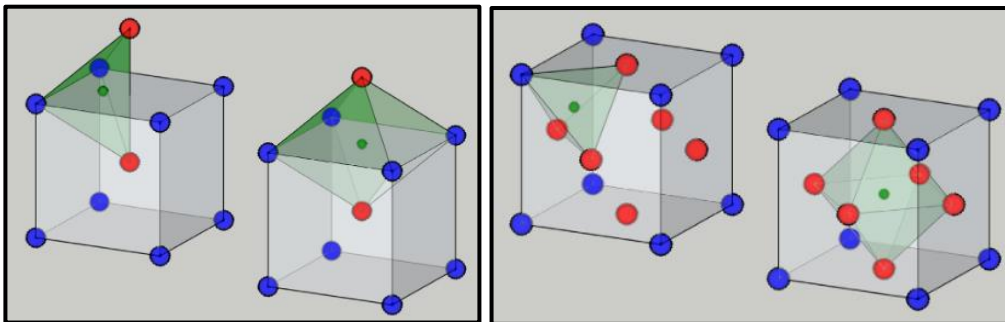


Figure 3: Diagrams of the BCC (left) and FCC (right) crystal structures. The tetrahedral sites are on the left in each image. The green sphere represents the dissolved proton occupying an interstitial site in the unit cell [2].

The diffusion aspect of solution-diffusion hydrogen transport is not as well understood. Several mechanisms for how protons move through a metal lattice have been proposed, but those of Kehr are considered the most robust. He proposes four different temperature dependent diffusion mechanisms. At low temperatures, in the absence of thermal vibrations, hydrogen atoms become trapped within the relaxed lattice. The “self-trapped” atoms must move to the adjacent interstitial site via a quantum mechanical process known as “band propagation”. As temperature increases, hydrogen atoms begin to move via thermally activated tunneling pathways that require the presence of thermal vibrations also known as phonons. In the third temperature region, the hydrogen atoms can be modeled as classical particles that can perform over-barrier jumps between interstitial sites. Finally, in the highest temperature region the hydrogen atoms begin to behave in a fluid-like manner and are no longer confined to interstitial sites. Given the operating temperature of most metal membranes (200-600°C), temperature region three is of the most interest to this work [2].

Theoretical models like density functional theory have been used in combination with experimental data to predict the diffusion behavior of hydrogen in metals. For example, the rate of thermally activated jumps, which constitutes Kehr’s proton diffusion mechanism of interest, can be calculated using the vibrational frequencies of interstitial sites and the difference in energy between interstitial and transitional sites within the lattice. Using these calculations, it was shown that at typical metal membrane operating temperatures (~400°C) hydrogen diffusion was dominated by thermally activated jumps. These findings are in agreement with the research of Kehr [2].

In dense ceramic membranes, protons move in a different manner. Like palladium, certain oxides can dissolve significant concentrations of hydrogen at high temperatures. Protons then move through ceramic membranes via two principal mechanisms; the Grotthuss mechanism and the vehicle mechanism. With the vehicle mechanism, the proton moves as a passenger attached to a larger ion such as NH_4^+ or OH^- . The Grotthuss mechanism involves the movement of protons between relatively stationary host anions. The materials studied in this work conduct protons via the vehicle mechanism with hydroxide ions acting as the vehicle [7].

1.5. Mixed Ion Conducting Membranes

Mixed ionic-electronic conducting (MIEC) membranes are materials that conduct matter in the form of ions or atoms and electronic charge carriers as holes or electrons. In addition to true MIECs there are heterogeneous MIECs which are composed of a mixture of two phases. One phase conducts the ions while the other acts as the electronic conductor. The two main ionic species which MIEC's transport are protons and oxygen ions. MIEC's ability to conduct electronically requires the use of electrodes to avoid the creation of an internal short circuit. The ionic component of an MIEC's conductivity requires a pressure gradient through the material. For example, to conduct oxygen ions there must be a difference between the O_2 gas partial pressure on either side of the membrane. The oxygen ions will move from higher partial pressure to lower. An absence of external electrical connections means the net current through the membrane is zero therefore, the flow of oxygen ions must be countered by the flow of electrons in the opposite direction. This same principle can be applied to separate hydrogen from a mixture of gases in a MIEC [8] [9].

MIECs have many interesting applications due to their ability to separate hydrogen and oxygen at near 100 percent purity. High purity oxygen is useful for various medical applications and in the production of syngas. These materials can also be incorporated into catalytic membrane reactors to intensify certain petrochemical processes. As was mentioned before, more sustainable and cheaper methods for hydrogen production are highly desirable. In one possible scheme, MIECs are used in conjunction with the water gas shift reaction such that hydrogen generation and separation via an MIEC membrane are combined into a single reactor. MIECs may also be used in tandem with proton conductors to create composite configurations for application in specialized membrane reactors. The two conductors would allow for the passage of protons or oxygen ions to opposite sides of the membrane to be utilized as reduction or oxidation agents. These are both examples of how membranes can be utilized to intensify processes [9] [10].

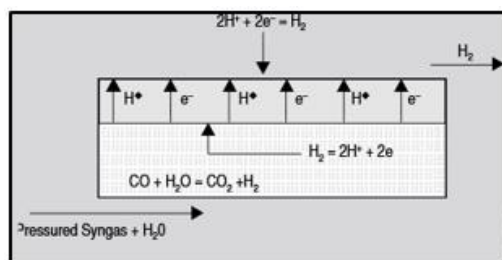


Figure 4: Schematic of mixed membrane reactor for production of pure hydrogen adapted from [9].

1.6. Defect Theory

A perfectly ordered solid inorganic compound is hard to find, as defects or imperfections exist in practically all of them. Their omnipresence can be attributed to the effect they have on the Gibbs free energy of the solid. According to the Gibbs free energy equation, an increase in entropy leads to a lower Gibbs free energy and a more stable compound. This increase in the entropy or disorder of the compound stems from all the possible positions in which a defect can exist. Defects serve an important purpose in these solids, as they provide a means for ions or electrons to diffuse through the lattice [10].

$$\Delta G = \Delta H - T\Delta S$$

Equation 3: Gibbs equation of free energy

Defects can be divided into two different classes, electronic and structural. Electronic defects arise from electron excitation into the conduction band or they are created when the electroneutrality of the solid is no longer balanced. While there are several different types of structural defects, the type most relevant to this work is the structural point variety. A point defect is defined as a structural position that contains an atom, ion or molecule that would not be present at that position in a perfectly stoichiometric material. A structural point defect could be an ion occupying a space that should be empty, a vacancy in a position which should be filled, or an ion with an abnormal charge. Oftentimes, researchers will mix different oxides to form solids with a higher concentration of defects to increase ionic conductivity [5] [10].

An understanding of defect concentration is important because of its effect upon the electronic and ionic components of a compound's overall conductivity. For a particular inorganic oxide, the conductivity depends on three factors: defect concentration, charge and mobility. Since the mobility values for electrons and electron holes are two to three

orders of magnitude greater than those of ions, the concentration of ionic defects must be 1000 times that of electronic defects to make the material a true ionic conductor. In non-stoichiometric oxides, the concentration of electronic and structural defects changes with both temperature and gas partial pressure (hydrogen or oxygen). Consequently, certain oxides may be predominantly ion conducting at one set of conditions and electronic at another [10].

2. Objectives

The overarching objective of this work is the development of thin film conductors with low ionic resistance for application in separation processes. Several specific goals were chosen with the aim of satisfying this principal objective. The first goal is to obtain a dense and homogenous proton conducting metallic thin film consisting of a layer of palladium on top of a porous ceramic membrane. All films are deposited via the sputtering physical deposition process. This objective will coincide with the electrochemical and structural characterization of a sputtered film of calcium doped gadolinium oxide. The electrochemical characterization is employed to determine what type of conduction dominates through the GCO layer – protonic or electronic. This characterization is also useful to determine how the conditions – water partial pressure and temperature – affect the conductivity of the thin film. Following these two sub-objectives, a final step is to develop a composite proton conductor consisting of a layer of GCO deposited between two thin films of palladium. The goal of this final step is to obtain a homogenous, densified layer of GCO over the bottom layer of sputtered palladium. After the structural characterization, the dual membrane will be ready for electrochemical characterization via permeation testing.

This project also seeks to develop a composite membrane consisting of a mixed ion conducting membrane thin film deposited onto a proton conducting substrate. The mixed ion conductor and proton conductor are gadolinium doped ceria oxide and BCZYYb respectively. The concrete goal of this stage is to obtain a dense, homogenous film of CGO on top of the BCZYYb substrate. The CGO films are also deposited via sputtering.



3. Experimental Methodology

3.1. Material Synthesis

In this thesis, many of the materials were bought commercially either as powders or in a ready-to-use form. Certain materials were prepared in house such as the calcium doped gadolinium oxide, which was synthesized via the co-precipitation route.

3.1.1. Co-precipitation

Co-precipitation is a useful method for the synthesis of nanometric sized powders. The method was employed in this work for the formation of calcium doped gadolinium oxide. For the formation of this compound the first step is to prepare a mixture of commercial calcium and gadolinium nitrates in deionized water. An ammonium carbonate solution is then added to the nitrates to incite full precipitation. The resultant precursor powder is then filtered, rinsed and dried at 150°C [11].

3.2. Material Selection

The following is a summary of the principal materials used in this masters thesis

3.2.1. Gadolinium Doped Cerium Oxide (CGO)

Cerium oxide is an inorganic solid which adopts the fluorite structure and exhibits n-type electronic conductivity. The fluorite ceria is very tolerant to mixing with other oxides. Due to this flexibility, there has been much research in the way of doping cerium oxide to change its conductive properties. One popular group of dopants are the rare earth elements. Doping with this group of oxides has a significant effect upon conductivity of the solid because for every two trivalent rare earth cations incorporated into the ceria oxide structure, an oxygen vacancy is introduced. In accordance with defect theory, ionic conductivity will be increased upon the formation of oxygen vacancies [12].

Despite its promotion of ionic conductivity, acceptor doping has been shown to cause straining in the cerium oxide lattice. This type of deformation is referred to as chemical expansion and it results in mechanical stresses that negatively affect conductivity and can cause structural failure. To minimize the chemical stress factor, rare earth cations that are most similar in size to the cerium cation are chosen. Of the rare earth oxides, gadolinium provides the lowest size mismatch and is a popular dopant to increase ionic conductivity in cerium oxide [12] [13].

Cerium oxide doped with gadolinium possesses a combination of interesting properties such as high oxygen-ion mobility, redox catalytic properties and resistance to water and carbon dioxide. Given these properties, CGO has been studied for application as an electrolyte for intermediate temperature solid oxide fuel cells and as a mixed-conductive membrane for oxygen separation [13].

In this work, commercially bought cerium oxide powder with a 10% dopant content of gadolinium oxide is used. The following is the stoichiometry of the mixed oxide compound, $\text{Ce}_{0.9}\text{Gd}_{0.1}\text{O}_{3-\delta}$. The CGO powder is pressed into a disc and then sintered for 10 hours at 1300°C to be employed as a sputtering target.

3.2.2. Palladium and Alloys

Palladium is a rare and lustrous silvery-white metal that is considered a member of the platinum group. It is soft and ductile when annealed and has a relatively low melting temperature. The largest use today of palladium is in catalytic converters because of its ability to convert up to 90% of harmful gases in automobile exhaust. Palladium is also popular for making jewelry and surgical instruments. In this work, palladium is exploited as a selective hydrogen separation membrane [4].

Many metals are capable of selectively transporting hydrogen at high rates. Materials such as Nb, V and Ta have permeability values greater than that of palladium, but their tendency to form oxide layers makes them difficult to use as membranes. Palladium possesses certain properties that make it ideal for the purpose of hydrogen separation. For one, palladium has a catalytically active surface for hydrogen splitting. Although hydrogen can diffuse rapidly through other metals, these metals lack the catalytic activity to split atmospheric hydrogen into the protons which dissolve in the metal. This causes these metals to have low rates of absorption and desorption and the entire separation process is hindered. Another distinct advantage of palladium as a hydrogen membrane is its ability to absorb large volumes of hydrogen. In 1866, Thomas Graham conducted experiments using palladium foils and discovered that the metal could absorb 600 times its own volume in hydrogen without compromising its physical properties or structural integrity [2] [4].



When hydrogen dissolves in palladium a pd-h system is formed. This system may exist in two different phases depending on temperature and the H/Pd ratio. Both phases are interstitial solid solutions and they are referred to as the alpha (α) and the beta (β) phases. The two phases maintain the same FCC crystal structure as pure palladium but with longer lattice parameters. When the protons dissolve in the metal the lattice parameters increase from 0.3890 nm to 0.3895 nm for the α phase and up to 0.410 nm for the β phase at ambient temperature. At lower H/Pd ratios and higher temperatures the α phase is dominant while the β phase takes over at higher H/Pd ratios and coexists with the α phase at lower temperatures. A diagram showing which phases exist at different temperatures and hydrogen percentages is presented in figure 5. The volume change which the material undergoes upon phase transition can cause strain and recrystallizations leading to bulk and grain boundary defects. Another issue palladium membranes experience when exposed to hydrogen atmospheres is a loss of ductility. This phenomenon has been deemed “hydrogen embrittlement” and compromises the membrane via cracks in the metal [1] [2] [4].

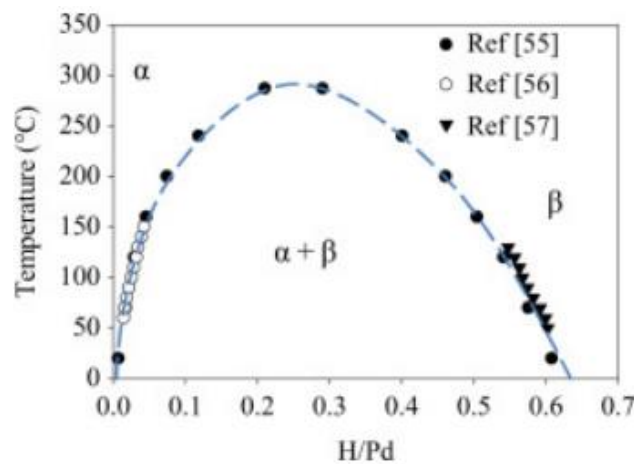


Figure 5: Palladium-Hydrogen system phase diagram [2]

One way in which investigators are tackling phase change and embrittlement complications is by alloying palladium with other metals. A membrane consisting of 23% silver has been found to lower the critical temperature of the alpha-beta phase change from 298°C to room temperature. This allows for lower more sustainable membrane operating temperatures. Most importantly, the alloyed membrane maintains the permeability and selectivity of a pure palladium membrane. Another widely studied binary system is that of palladium-copper. Research has shown that palladium-copper membranes do not exhibit the embrittlement effect even at ambient temperatures. Furthermore, the substitution of cheap copper metal for expensive palladium leads to significant cost savings. Palladium-gold alloyed membranes also reduce embrittlement

and exhibit increased resistance to catalytic poisoning by various sulfur compounds. However, the cost of gold is an obstacle in the way of wide spread implementation of palladium-gold alloyed membranes [1].

The metallic targets used for sputtering in this study were bought commercially from Merck Company and all were of at least 99.95% purity. In figure 6 a photo of the silver and palladium targets are shown alongside their original packaging.



Figure 6: MaTeck metallic palladium and silver targets used for sputtering deposition

3.2.3. Calcium Doped Gadolinium Oxide (GCO)

Gadolinium Oxide is an inorganic crystalline compound with the formula Gd_2O_3 . The oxide is one of the most commonly available forms of the rare-earth element gadolinium. Gadolinium oxide possesses crystallographic stability up to $2325^{\circ}C$, high mechanical strength and excellent thermal conductivity. Oxides such as this are useful as high temperature proton conducting solid electrolytes for applications in hydrogen sensors, fuel cells, water vapor electrolysis and electrochemical reactors for hydrocarbon conversion [14].

The compound is classified as a sesquioxide due to the ratio of gadolinium atoms and oxygen atoms within the crystal structure (3:2). The compound can adopt three different crystal structures, cubic, monoclinic and hexagonal. In this work, operation temperatures do not exceed $1200^{\circ}C$ and the oxide remains in its cubic form. As was mentioned earlier, rare earth oxides are capable of dissolving significant quantities of protons in the presence of water vapor or hydrogen at high temperatures. In structures such as these, the dissolved protons form hydroxide defects at oxygen sites with an

effective positive charge. The dissolved protons diffuse through the oxide attached to hydroxide anions in a process deemed the vehicle mechanism. In this work, calcium is added to the gadolinium oxide to act as an acceptor dopant. When incorporated into the crystal structure, the acceptor dopant forms a defect with an effective negative charge which must be compensated by positively charged defects from protons, oxygen vacancies or electron holes. Norby has demonstrated in several studies that at lower temperatures and high water vapor pressures, protons are the dominating defects while at higher temperatures and drier conditions native defects, assumed to be oxygen vacancies, take over [14] [15] [16].

In this work GCO powder with a stoichiometry of $G_{1.98}C_{.02}O_{3-\zeta}$ was synthesized via the coprecipitation method. The powder was pressed into a solid disc and then sintered for densification. The resulting disc was suitable to be used as a target in an RF sputtering machine.

3.2.4. Substrates

The following are the materials which were used as substrates to support the deposited thin films. All substrates were ultrasonically washed in isopropyl alcohol and water for 10 minutes each before deposition to ensure complete cleanliness.

3.2.5. BCZYYb

Barium Cerate Zirconia co-doped with Yttrium and Ytterbium (BCZYYb) is a proton conducting ceramic oxide with interesting properties related to resistivity and conductivity. The oxide is based on a barium cerate-zirconate system which combines the high protonic conductivity of barium cerate with the atmospheric stability of barium zirconate. In 2003, the first studies were performed with the co-doped barium cerate-zirconate oxides and it was found to have an ionic conductivity 2 times higher than that of the material singularly doped with Y. Furthermore, BCZYYb exhibits fantastic stability when exposed to sulfur and coking atmospheres. This resiliency makes them a material of interest for hydrocarbon applications. It has been hypothesized that this increased stability lies in the dissociated adsorption of water on the surface of BCZYYb. The dissociated water helps to oxidize adsorbed sulfur compounds [17].

One of the main issues with BCZYYb is its sinterability. To create a fully densified material, exposure to extreme temperatures above 2000°C for over 24 hours is required. These long and hot sintering processes can cause barium volatilization, which leads to the formation of secondary phases and a lower overall conductivity. To combat the

sintering problem, several sintering aids have been explored. Some examples include zinc oxide, tin oxide and nickel oxide. In this work, nickel oxide is added as a secondary phase. Nickel compounds are useful to improve grain growth and densification during sintering while having a negligible effect on conductivity. Another reason for the addition of the nickel in this work is to add electronic conductivity to the material [17].

In this thesis BCZY was bought as a commercial powder doped with Yb and mixed with nickel. This powder was pressed into a disc and sintered at 1600°C for 36 hours.

3.2.6. Commercial Ceramic Membranes – Anodisc/A-tech

In this thesis two porous ceramic membranes were used as supports for the thin metallic films. SEM images of the surfaces of the two substrates can be seen in figure 9. Anodisc is an alumina based thin and delicate substrate that consists of two faces with dissimilar characteristics. For the depositions performed in this work the top face is utilized. It contains an outer ring with pores around 200 nm in diameter. The inner circle consists of regularly distributed 20 nm pores.

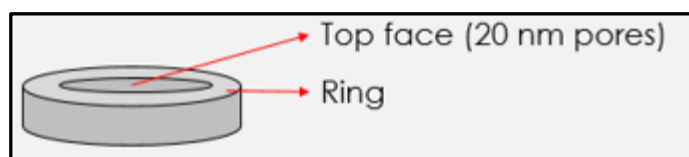


Figure 7: Schematic of Anodisc substrate

A-tech is a similar alumina-based membrane but is thicker and sturdier than the Anodisc material. The A-tech substrate consists of two different phases of alumina oxide. A thin phase with smaller pores is deposited on top of the bulk phase. The face with the thin phase is the one which is used as the deposition surface. Both phases are visible in the cross-sectional image in figure 8.

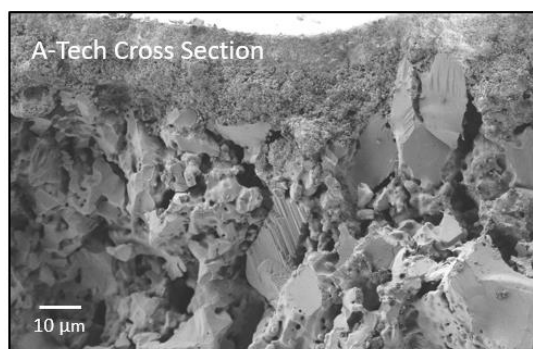


Figure 8: SEM image of a cross section of the A-tech substrate. Both phases are visible. The top of the image is used as the deposition surface.

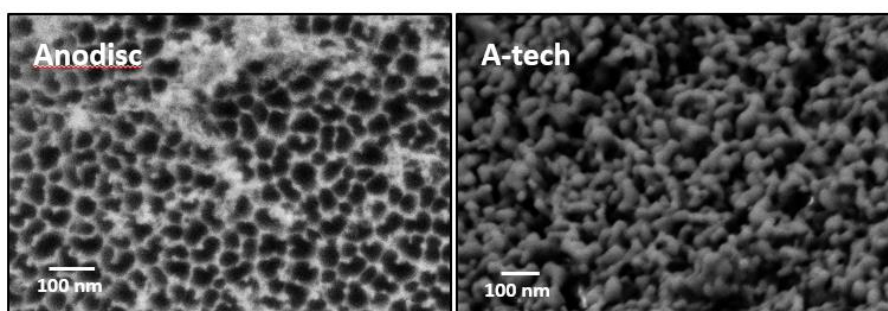


Figure 9: SEM images of the faces of the two ceramic substrates used as surfaces for sputtering deposition.

3.3. Sputtering

Sputtering is a thin film deposition technique in which atoms are ejected from a “target” material and deposited on a substrate in a plasma environment. The sputtering process begins when a substrate and target are placed in a vacuum chamber. Once the chamber is evacuated to eliminate contaminants and background gasses, a sputtering gas of which the plasma will be comprised is introduced. To initiate plasma generation, a high voltage is applied between a cathode behind the target, and an anode. Electrons within the sputtering gas are forced away from the cathode and subsequently collide with the atoms of the inert sputtering gas causing them to be ionized. The positively charged sputter gas atoms now accelerate towards the negatively charged cathode and collide with the target. This “bombardment” of the target with the sputter gas ions causes the ejection of atoms on the surface of the target into the vacuum environment. The ejected target atoms then travel through the chamber and are deposited onto the substrate to form the thin film [18].

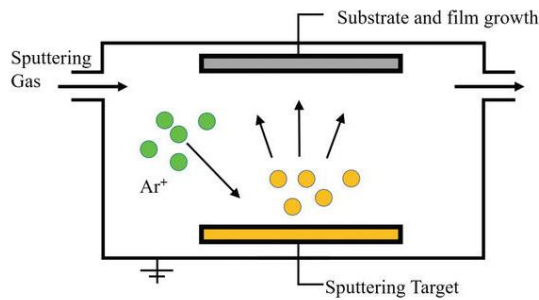


Figure 10: Simple schematic of a magnetron sputtering chamber [18]

In this work, a variation on the traditional DC sputtering method called Radio Frequency (RF) Sputtering is utilized. RF sputtering allows for the use of insulating target materials such as oxides and ceramics. When performing DC sputtering with insulating targets, the positive gas ions will inevitably accumulate on the surface of the target and the bombardment by further ions will be suppressed. RF sputtering alleviates the charge build up by alternating the electrical potential. This allows the surface of the target to be periodically “cleaned” of the charge build up. There are two cycles in RF sputtering. During the positive cycle, electrons are attracted to the cathode and therefore to the target material as well. When the cycle enters its negative phase, the bombardment of the target with positive sputter gas ions resumes and deposition continues [18].

The sputtering set up used for this thesis consisted of a Pfeiffer Classic 250 turbo molecular pump for chamber evacuation, two Cesar power generators as energy sources and three available magnetrons. All depositions were done in a vacuum environment and a five-minute pre-sputtering step was always performed to clean the target before bombardment.

3.4. Characterization Methods

3.4.1. X-ray Diffraction

X-ray diffraction (XRD) is a nondestructive structural characterization technique used to obtain information about the crystal structure of a solid material. This information includes identification of crystalline phases and their orientation, lattice parameters and crystal size.

By definition, a crystalline material contains atoms arranged in a repetitive pattern. The smallest repeating unit within a crystalline material is called the unit cell. The unit cell repeats in all three dimensions to form the given crystalline material. A unit cell can be described by the length of the cell edges (a,b,c) as well as the angles between them (α , β , γ). Combinations of these 6 parameters yield fourteen distinct types of unit cells, they are called the Bravais lattices [11].

XRD begins when a monochromatic x-ray beam meets a crystalline sample at a given angle. When a focused x-ray beam encounters the atoms part of the beam is transmitted, part of it is absorbed, part of it is scattered and part of it is diffracted. The part that is diffracted is what is harnessed to obtain the desired information. Depending on how the atoms are arranged in the crystal lattice the x-rays will be diffracted differently. The diffraction pattern is recorded via a detector and is then analyzed to obtain the “fingerprint” of the material [12].

The XRD measurements for this work were done using a Cubix fast diffractometer employing CuK α radiation ($\lambda_1 = 1.5406 \text{ \AA}$, $\lambda_2 = 1.5444 \text{ \AA}$, $I_2/I_1 = 0.5$) and an X'Celerator detector in the Bragg-Brentano geometry. Diffraction patterns were analyzed using the X'pert Highscore Plus software.

3.4.2. Scanning electron microscopy

Scanning electron microscopy is a popular method for the production of high-resolution surface images. SEM involves the generation of high energy electrons via a heated tungsten filament. The electrons scan the surface of the sample as a beam and as they interact with the atoms various signals are produced. The topographical and compositional information contained within the signals is collected and used to form an image. SEM is capable of magnifying samples up to six orders of magnitude and allows for a relatively large depth of field [12].

The principal microscope used for the SEM images presented in this thesis is the Zeiss Ultra55 field emission scanning electron microscope (FE-SEM) with an acceleration voltage up to 30 kV [19].



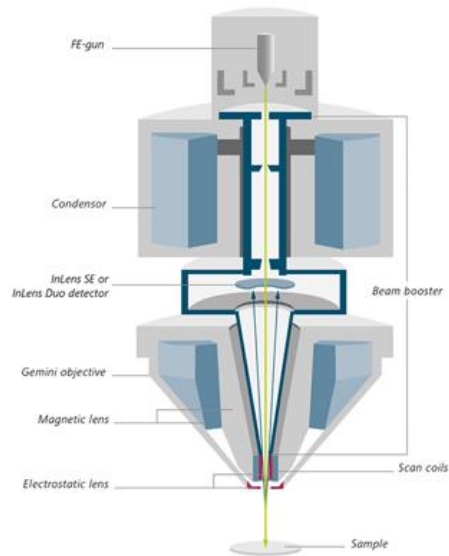


Figure 11: Schematic of Field Emission Scanning Electron Microscope [19].

3.4.3. Energy Dispersive X-ray Spectroscopy

Energy dispersive x-ray spectroscopy (EDS) is both a quantitative and qualitative chemical microanalysis technique which is used in conjunction with SEM. EDS uses the x-rays that are emitted from the sample when it is exposed to the SEM electron beam. Using both SEM and EDS together provides information about both the sample morphology and the chemical composition of the different phases present. Minimum detection limits range from 0.1 weight percent to up to three percent depending on the element and the matrix being analyzed [12].

EDS microanalyses were performed with the FE-SEM microscope with a detector from Oxford instruments. The software INCAEnergy/Wave was used to interpret the x-ray patterns obtained during EDS analysis.

3.4.4. Electrochemical Characterization

The electrochemical characterization of the sputtered thin films was done via conductivity measurements using the direct current 4-point configuration. The 4-point configuration is advantageous over 2-point measurements because it eliminates the influence of contact and wiring resistance.

In this method, silver wire contacts are applied to the thin film sample using silver paste. During the measurements, a continuous current ramp is applied to the sample between the two external contacts. This coincides with the measurement of the difference in potential between the two internal contacts. To eliminate the thermal effect and avoid non-ohmic responses the current is applied in both directions. The conductivity measurements are taken within a temperature range between 25°C and 800°C. Before beginning the measurements, the sample is maintained at 800°C for 12 hours to ensure stability. After confirming stability, the temperature begins to decrease at a rate of 2 degrees per minute while measurements are recorded every two minutes. A diagram of a 4-point measurement set up on a thin film sample is shown in figure 13 [5] [12].

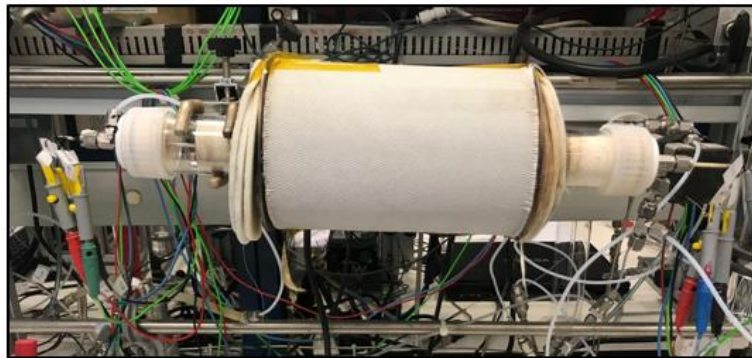


Figure 12: Chamber in which conductivity measurements are performed under different atmospheric conditions

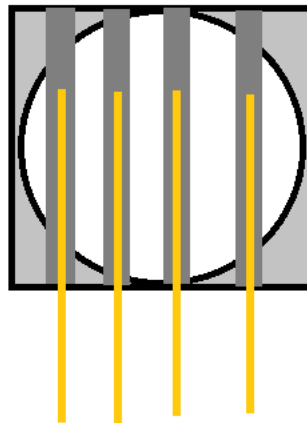


Figure 13: Schematic of thin film sample prepared for 4-point conductivity testing. The white sphere is the thin film on top of the grey square substrate

These electrochemical measurements were carried out in 4 different sets of conditions. The atmospheres to which the samples were exposed during measurement were as follows: 5% percent hydrogen and 95% argon in a dry atmosphere, 5% hydrogen and 95% argon in a wet atmosphere, 5% deuterium and 95% argon in a dry atmosphere, 5% deuterium and 95% argon in a heavy water atmosphere. The reason for conducting measurements under different conditions is to determine which type of conductivity dominates (protonic or electronic) through the thin film. The method itself will only give information about the total conductivity of the sample [5].

Measuring in both D₂ and H₂ environments allows for the observation of the isotopic effect. The isotopic effect is a very useful tool for qualitatively confirming the protonic nature of a solid oxide conductor. Since deuterium has a mass two times larger than hydrogen, it diffuses more slowly through the film. Therefore, if the proton is the dominant charge carrier in the material, the conductivity in the D₂ atmosphere will be noticeably lower than in the H₂ environment [5].

4. Discussion of Results

4.1. Palladium membranes

Palladium is capable of being a highly selective hydrogen membrane which conducts protons via the solution-diffusion mechanism. Any pin-hole or similar defect in the palladium layer would cause for the passage of undesirable gas species rendering the membrane useless. Therefore, it is paramount that a palladium layer is obtained that is completely dense. Attaining such a layer is complicated due to the presence of surface defects on the substrate, and the pinholes which are an unfortunate byproduct of the RF sputtering technique. The process of achieving a densified membrane involved the use of different substrates, post processing techniques and deposition conditions. The results of the palladium deposited on the A-tech substrate will be discussed first.

During the sputtering deposition there were three variables available for manipulation; deposition time, temperature, and gas flow. The first depositions were done for 1 hour with 40 sccm flow of Argon at 400°C and 550°C. The SEM images in figure 14 show the presence of multiple pinholes and gaps between the grains. This strongly suggests that the layer is not dense. Note that depositing at 400°C resulted in more tightly packed grains than when depositing at 550°C. According to these images, it seems that one hour of deposition was not sufficient for the creation of a dense layer. An increase in



deposition time would allow for more film growth and may help to cover the pinhole defects.

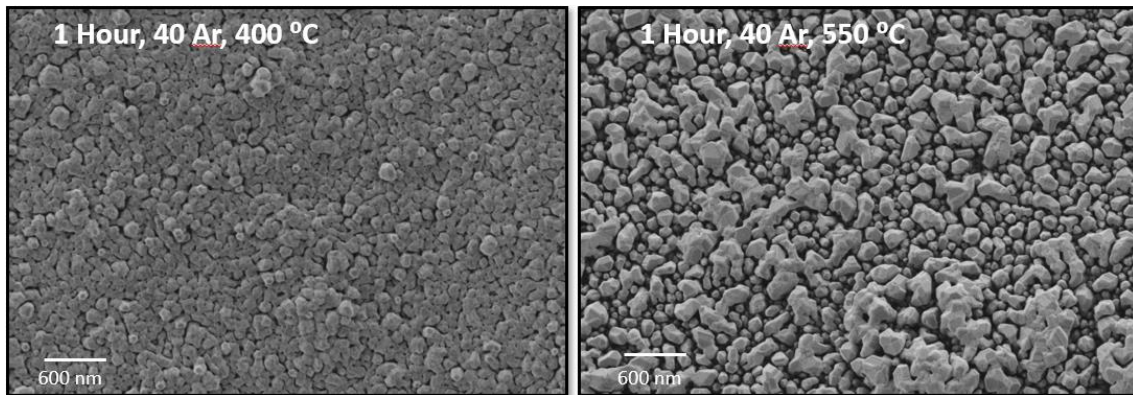


Figure 14: SEM images of palladium deposited on top of a-tech substrate at different temperatures

The sputtering deposition time was increased five-fold for a total time of five hours for all future samples. Furthermore, room temperature depositions were added to further narrow down the optimal temperature range. In figure 15 are three images of thin films deposited for five hours with an argon gas flow of 20 sccm. At room temperature the palladium forms cauliflower-like shapes. The cauliflower like shape was observed for all samples sputtered at ambient temperature. This type of film morphology indicates a very porous layer and calls for the exclusion of room temperature from the optimal range.

Once again, it can be observed that at a temperature of 400°C a more favorable layer is produced with tighter grain packing than at 550°C. It is probable that between 400°C and 550°C the layer undergoes a substantial physical change and upon cooling it loses its desired properties. Either way, these images are conclusive in determining 400°C to be within an acceptable temperature range for producing the optimal thin film. Nonetheless, a fully dense layer has still not been achieved as pinholes are located throughout the film and small borders exist between some grains. Flow of argon remains the final sputtering condition which is yet to be explored.

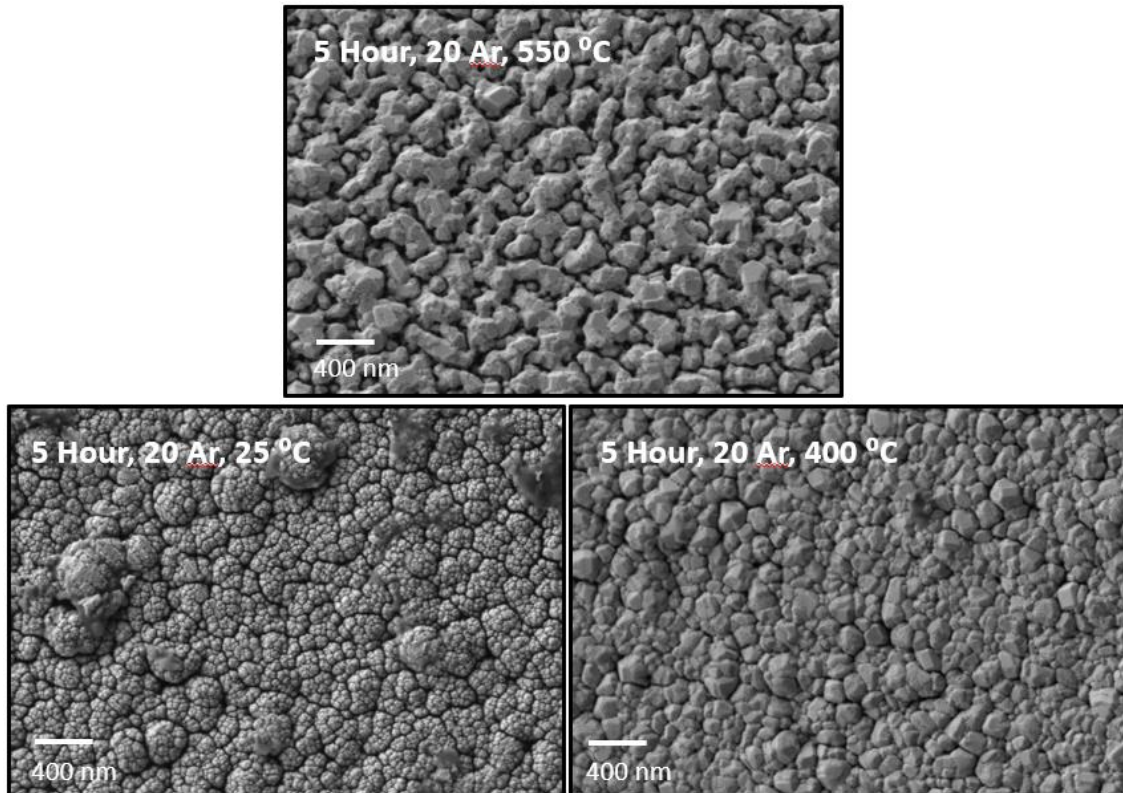


Figure 15: SEM images of palladium thin films at various temperatures after 5 hours of sputtering deposition

Using the optimal temperature of 400°C, argon gas flow was doubled from 20 sccm to 40 sccm while maintaining a deposition time of 5 hours. Previous studies on the effect of argon gas partial pressure on metallic sputtered thin films have found that increased argon gas flow promotes crystallinity and leads to an increase in grain growth. This experiment supports that claim as the increased gas flow results in the most desirable layer yet. In reference to the images in figure 16; there are minimal gaps between the grains and the morphology of the film is far more homogenous than it was at the lower argon partial pressure. Still, many small pinholes with diameters between 50 and 90 nm are spread throughout which suggests that the film is porous. A reference test was performed to qualitatively determine the level of porosity in the film. In this test the film is exposed to a liquid (acetone) and the time which it takes for the liquid to dissipate is recorded. The test is then carried out using a sample of a material which is known to be completely dense, and the two times are compared. The results of the experiment confirmed the non-density of the film. Nonetheless, this film held the acetone significantly longer than the other samples prepared under different conditions [20].

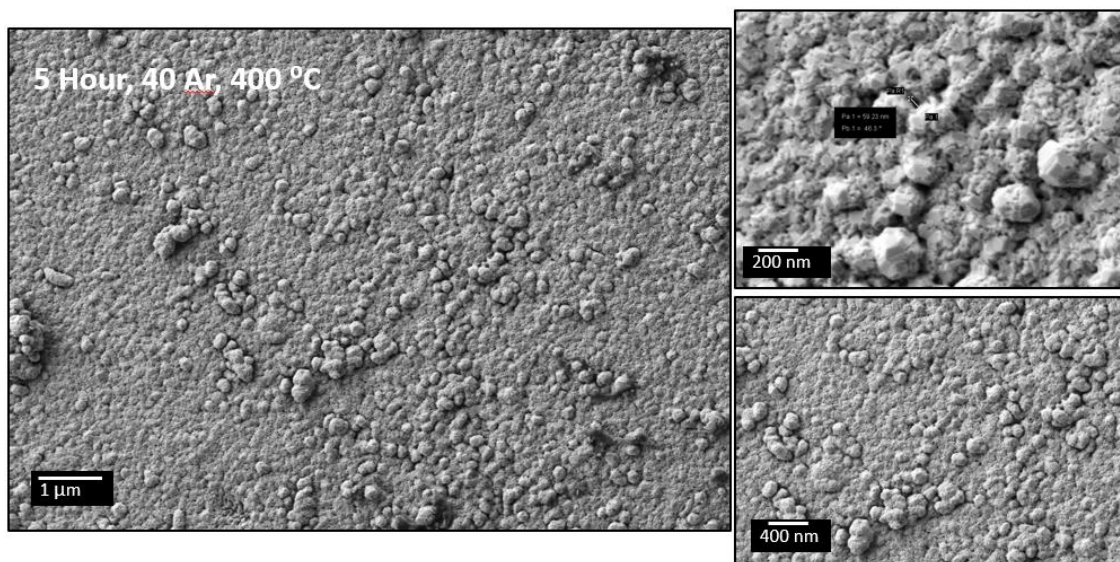


Figure 16: SEM images of most desirable thin film obtained with no post processing or alloying performed

After exhausting combinations of different sputtering conditions, the next step was to utilize post processing techniques to induce desirable morphological changes. The technique employed was annealing. The goal of the annealing step was to create a more conformal film by increasing grain size and releasing deposition related stresses. The annealing conditions chosen were 500°C in hydrogen gas for 2 hours with a 2 degree/minute temperature ramp for both the warming and cooling periods. In figure 17 an image of the annealed sample presents a densified thin film. Thermal treatment in reductive conditions incited film densification and resulted in a more conformal film.

Although the annealing step was successful, a new problem arose related to the adhesion of the palladium layer to the ceramic substrate. After annealing, with this sample and several others, the thin film delaminated from its substrate. The film at first appeared to be loose and then would delaminate in one solid piece from the substrate. The delamination was possibly due to differences in thermal expansion coefficients of the substrate and thin film. The lattice expansion typical of the alpha-beta phase change in the pd-h system may have also contributed to the poor adhesion. Despite the delamination problem, the results of the annealing complete the blueprint on how to obtain a densified sputtered thin film of palladium. A separate set of experiments should be carried out so that the thin film may maintain adhesion through the annealing process. A thin film with the morphology displayed in figure 17 is ready for the next stage of electrochemical testing.

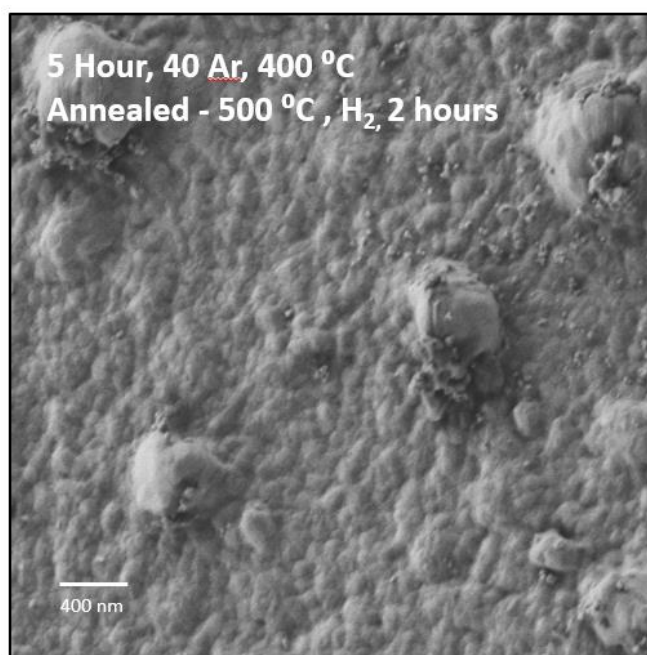


Figure 17: SEM image of annealed and seemingly densified palladium thin film

To overcome the issue of thin film delamination, the palladium was alloyed with copper and silver. The alloyed films were deposited via co-sputtering in which one magnetron bombards the target with palladium and the other with silver/copper. Equal power was applied to each magnetron, but deposition rates vary between materials.

Past work has shown that copper and silver can alleviate the mechanical stresses associated with the alpha-beta phase transition and may help to equalize the thermal expansion coefficients of the thin film and the substrate. Deposition time was decreased to two hours as the substrate was being bombarded with atoms from two targets. The temperature and gas flow used were those of the optimal pure palladium layer from figure 17 (40 argon sccm, 400°C). The two most desirable alloyed thin films are shown in figure 18. In the case of the copper alloy a dense and rather homogenous film appears to have been obtained. With the silver alloy, there are several pinholes present. The quality of the copper alloyed film is possibly due to the metal's well-known ability to promote sinterability at relatively low temperatures. According to EDX measurements, the weight percentage of the copper and the silver were 0.5% and 3.6% respectively. This indicates that very little copper or silver is necessary to significantly impact the morphology of the sputtered thin film. For example, the film containing copper consists of grains which are more cubic in nature than those of the pure palladium film formed under the same conditions.

Annealing was carried out for the palladium-silver sample with the hope that it would densify like pure palladium film. As before, the thin film delaminated from the ceramic substrate. The copper alloyed sample in this stage is very promising and a sample should be prepared for electrochemical testing.

In addition to the metallic alloys, a co-sputtering deposition was performed with palladium and an 8YSZ ceramic target to see if it would maintain adhesion upon thermal treatment. Indeed, the film did not delaminate after the annealing step. The film also maintained electronic conductivity which suggests that the palladium particles were in contact with each other. Nonetheless, the film was porous and metal-ceramic composite materials may not hold the same hydrogen permeation properties as alloyed metal membranes

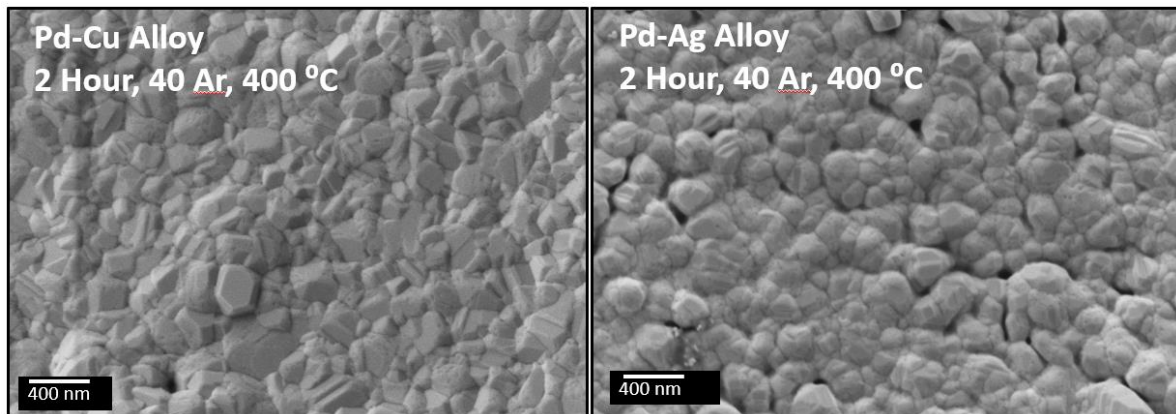


Figure 18: SEM Images of copper and silver alloyed thin films on A-tech substrate

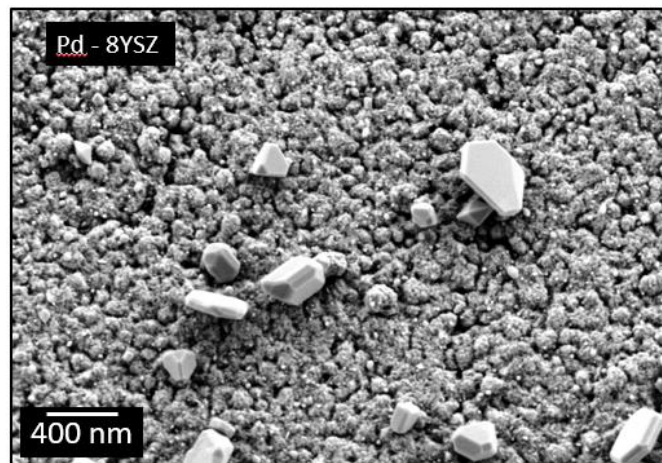


Figure 19: SEM image of the annealed 8YSZ-Pd alloyed film

A parallel study was also carried out using the Anodisc substrate. The results were similar to those of the films deposited on A-tech. In figure 20, note that depositing at room temperature once again produces a porous, cauliflower-like thin film. The optimal conditions for palladium deposition were confirmed in this study. The images show that at a higher gas flow rate and a temperature in the 300°C -400°C range the most desirable layer is created. The grains are more cubic on the optimal Anodisc sample than on the A-tech substrate. No annealing was performed with the Anodisc substrate as the material was found to deform during heat treatment. In the case of the Anodisc substrate, the goal of forming a dense layer has been achieved. The sample which is depicted in figure 20 on the right is set for electrochemical characterization via permeation testing.

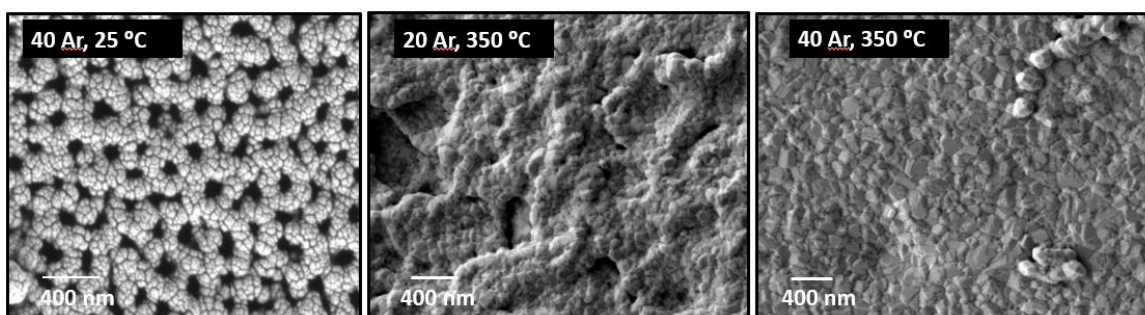


Figure 20: Images of thin palladium films deposited on Anodisc commercial substrate

4.2. GCO

Acceptor doped rare earth oxides such as GCO have been found to dissolve large quantities of hydrogen at both high temperatures and in atmospheres containing water vapor. The GCO thin films prepared in this section were deposited onto quartz substrates at 400°C for 10 hours. The only difference between the two deposition cycles was the argon gas flow which was 20 sccm and 40 sccm for the two samples. After the deposition, annealing was carried out in air at 800°C for 2 hours to ensure full crystallinity. The optimal deposition conditions and the subsequent annealing step were adapted from a previous work in which a desirable GCO layer was formed on quartz.

A limited structural analysis was carried out via XRD, the four diffraction plots can be seen in figure 21. The diffraction plots confirm the expected cubic structure of the oxide. A significant increase in peak intensity is observed upon annealing indicating an increase in crystallinity.

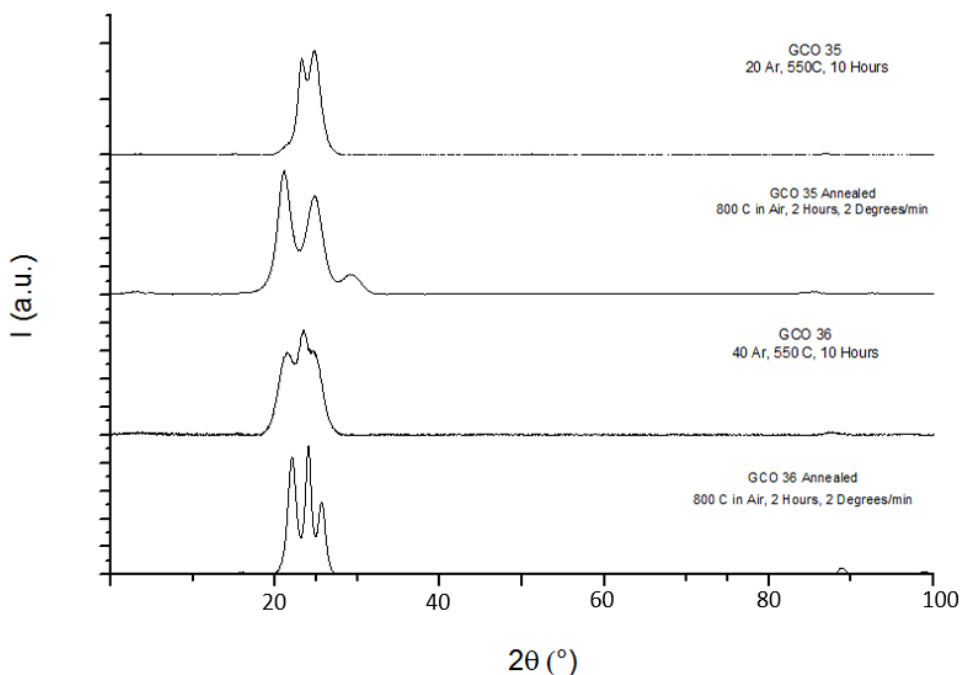


Figure 21: XRD plots of GCO thin film samples before and after annealing. The visible peaks correspond to the predicted cubic gadolinium oxide structure

In the end, the results of the four-point conductivity testing on the GCO thin films were inconclusive. The data did not show the expected proton conductivity which Norby and others had proved to exist in bulk acceptor doped rare earth oxides. The conductivity results were inconsistent between identical experiments and often erroneous. The four-point test is difficult to implement with thin film samples due to touching between wires and the possibility of the thin film rubbing off from the insulating substrate. The low electronic conductivity of GCO is an additional challenge as atypical current ranges need to be utilized. The electrochemical characterization of the rare earth thin films should not be abandoned as the nature of its conductivity in its thin film form is still not well characterized. Other applied current ranges should be explored, and new samples should be fabricated for testing to see if consistent and sensible results can be attained using the 4-point method. Another option available which could confirm the protonic conductivity of the GCO thin film is permeation testing. A configuration is explored in the next section which could be used for just this. However, a simpler configuration may be more sensible to minimize variability. Such a set up may consist of a GCO thin film between two easily applied porous electronic conductors acting as current collectors. A membrane like this could be used in experiments to test the hydrogen permeation of the GCO membrane and ideally characterize the GCO thin film as a proton conductor.

4.3. GCO on Palladium

After the GCO experiments, a membrane with a composite configuration was fabricated. The analyzed film consisted of a layer of GCO deposited on top of a thin film of palladium. Both the A-Tech and Anodisc substrates were utilized as supports in different samples. Characterizing this “open-faced” sandwich membrane is an initial step towards a final configuration of palladium-GCO-palladium. Leaving the GCO layer exposed allows for its analysis via SEM. In the completed sandwich membrane, the metallic palladium layers would act as current collectors while also permitting the selective passage of protons. The presence of the current collector is required because GCO has very low electronic conductivity and will not conduct protons without an applied current. An additional issue with supported dense palladium membranes is the interdiffusion of the metal film and porous substrate which can hinder hydrogen permeation, this is not the case with ceramic membranes. A simplified diagram of the two conductors in series working in a wet atmosphere is presented in figure 22 [21].

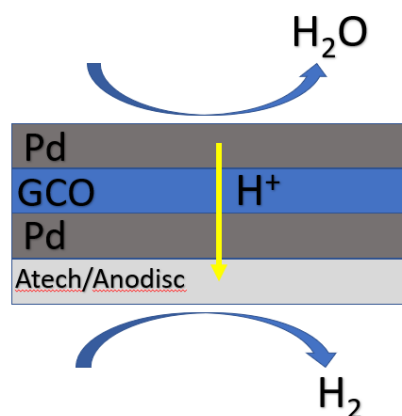


Figure 22: Simple schematic of protonic sandwich membrane operation

The goal of this stage of the work was to obtain a densified and homogenous layer of GCO on top of the palladium layer. The sputtering conditions for the palladium layer were those that produced the best pure metal film (40 Argon, 400°C, 5 Hours). The GCO layer was subsequently deposited in a separate run at 400°C for 5 hours with 20 sccm of argon. The conditions chosen for the GCO deposition were based on a previous work. In figure 23, SEM images of the open-faced sandwich membrane on A-tech are presented. Although the film has a rather homogenous particle distribution, many pinholes dot the film. Overall, the images show an irregular and porous layer unsuitable for application as a selective proton conducting membrane.

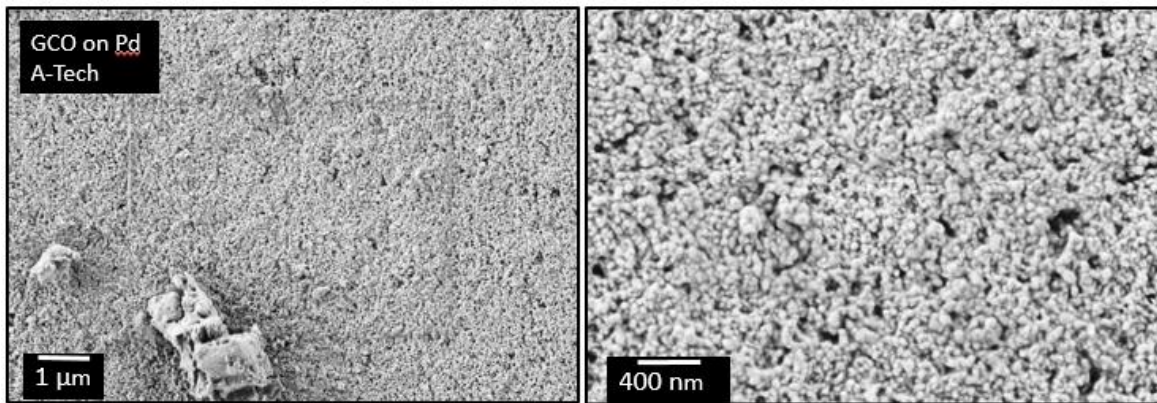


Figure 23: SEM Images of GCO deposited on top of palladium on the a-tech ceramic substrate

The composite membrane configuration was more successful when deposited onto the Anodisc substrate. The images in figure 24 show a dense cap, absent of pinholes, grain border gaps and defects. However, larger agglomerates of what are most likely GCO atoms compromise the homogeneity of the layer. The agglomerated particles suggest the presence of secondary nucleation sites created during the second deposition step. Nonetheless, these images are encouraging. The increased thin film quality could be attributed to the lesser roughness of the Anodisc substrate compared to A-tech.

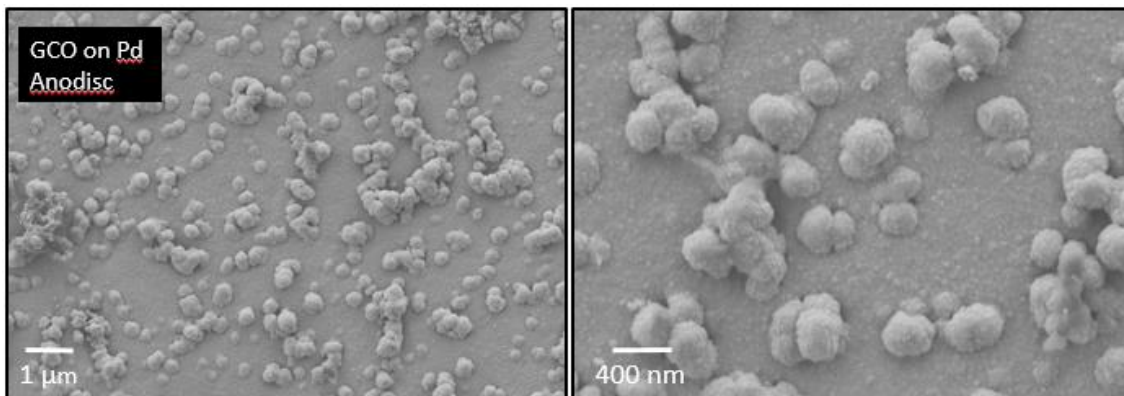


Figure 24: SEM images of GCO deposited on top of palladium on the Anodisc ceramic substrate

The sandwich membranes prepared in this stage were deposited on disc shaped substrates so that they may be measured in a permeation set up. Due to lack of time, these measurements were not performed, but the images here are very promising. One worry is that during electrochemical testing at high temperatures the thin film may delaminate, as was the case of the palladium membranes on A-tech. Another worry is that the deformation of the Anodisc material at temperature would compromise the integrity of the deposited cap. For this reason, it would be beneficial to further explore the possibility of depositing a desirable film onto the sturdier A-tech substrate. Either way, the results here are encouraging and the Anodisc sample is prepared for the next step of electrochemical characterization.

4.4. CGO on BCZYYb

Ionic and protonic conductors working in conjunction is a research area of interest for application in membrane coupled catalytic reactors and for use in electrolysis. The diagram in figure 25 is a simplified scheme of how these two types of conducting membranes could work in tandem. This would be an example of a catalytic membrane reactor for the conversion of carbon dioxide to methane. The membranes would act in parallel, serving to displace the reaction equilibrium and increase the performance of the reactor. The objective of this part of the study was to obtain a homogenous and densified thin film of the gadolinium doped cerium oxide ion conductor on top of a proton conducting BCZYYb substrate.

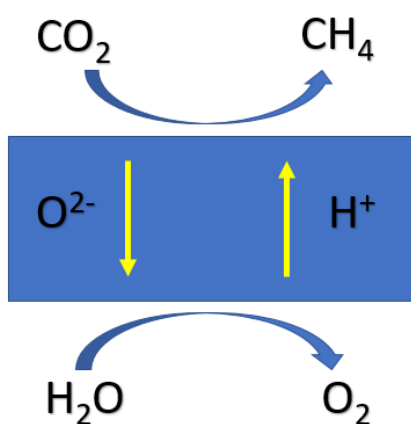


Figure 25: Schematic showing application for protonic and mixed ion conducting membrane working in tandem

During the CGO depositions, a gas flow of oxygen was added to the sputter chamber along with the argon. The introduction of O₂ gas is necessary to compensate for the lack of oxygen present during the vacuum sputtering process and allows the oxide films to approach their stoichiometric value [22].

The first CGO thin films formed showed evidence of secondary nucleation growth with irregular deposition and incomplete coverage. An SEM photo of one of these initial films is shown in figure 26. Although some areas are covered by the irregular particles, others remain completely bare, revealing the smooth substrate.

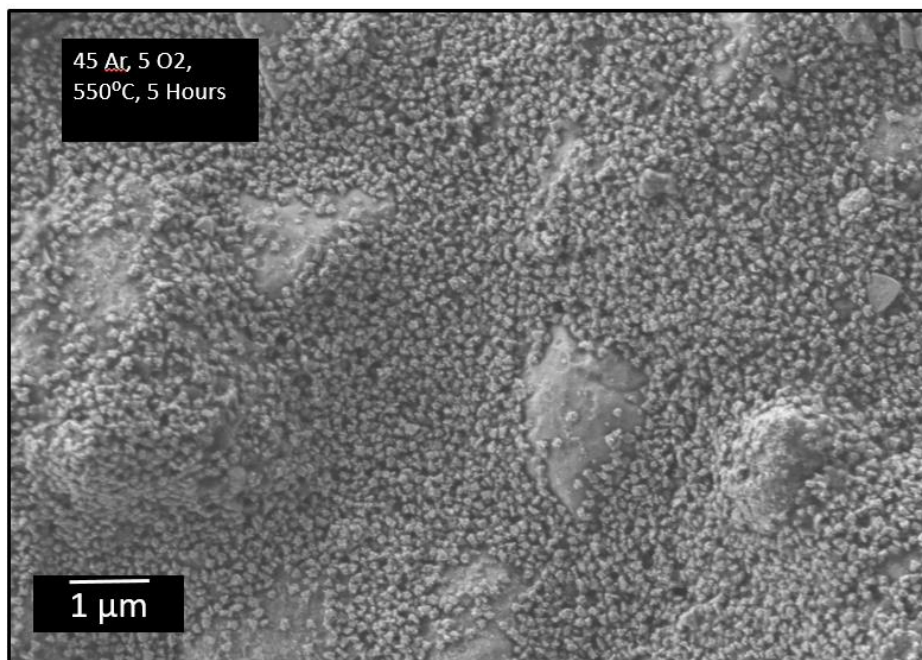


Figure 26: SEM image of CGO deposited on top of BCZYb substrate

In an attempt to obtain a more complete coverage, co-sputtering was carried out using two CGO targets on two different magnetrons. Both the magnetrons received the same power flow and theoretically should have been depositing at the same rate. The co-sputtering yielded better results with a more homogeneous and complete film. However, the presence of the larger irregular particles persisted, detracting from the homogeneity of the film. In figure 27, two images of the same co-sputtered sample in different areas are shown. In the image on the left, it is likely that there is a complete thin film with larger particles growing on top. However, in the image on the right it seems that the agglomerates are formed upon the bare substrate indicating an incomplete film. In both areas, a non-conformal film is observed

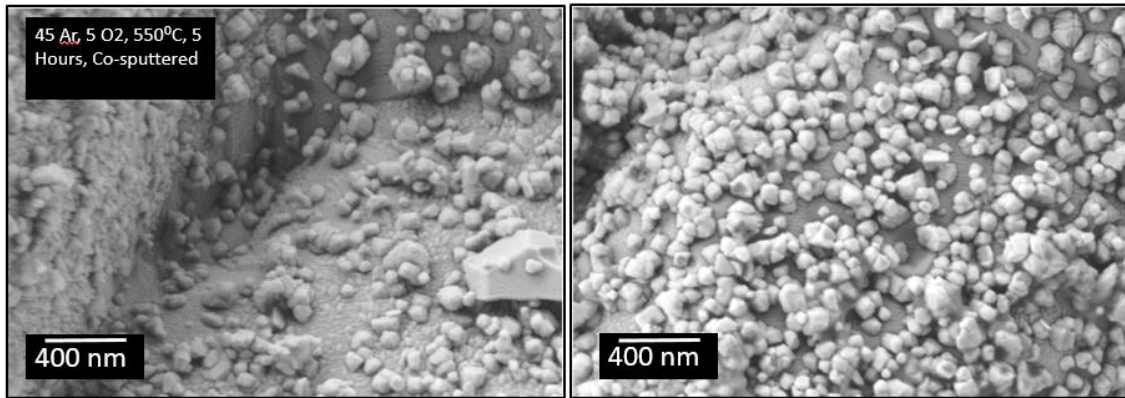


Figure 27: SEM images of CGO deposited on BCZYyb via co-sputtering with two CGO targets

During the co-sputtering depositions, it was suspected that one of the magnetrons was receiving less power and depositing at a lower rate than the other. To eliminate this uncertainty, depositions were done with one magnetron for double the time as the co-sputtering trials. The images of the single magnetron deposition in figure 28 are encouraging, as they show a rather homogenous film with spherical particles in certain areas of the sample. The morphology of the film is certainly distinct from that of the co-sputtered layer. However, observe in the landscape image on the right that several zones on the sample remain without coverage, exposing the bare substrate. Areas such as this are unacceptable if the objective is to be achieved. The increase in deposition time was done to assure that the lack of a desirable layer was not due to a shortage of time and a slow deposition rate. The images of these longer depositions show that an increase in time was necessary but also that further measures would be required to fulfill the objective.

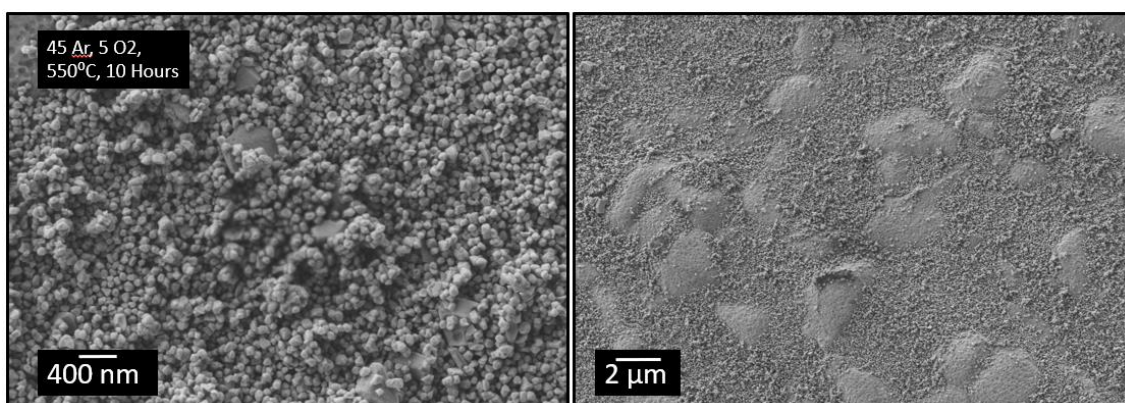


Figure 28: SEM Images of CGO film on BCZYyb for 10 hours with one magnetron

After analyzing the results of increased deposition time, a modification was performed on the substrate to incite better film growth. A thin layer of BCZY was screen printed on top of the BCZYYb/Ni substrate. The resulting two-layer substrate hoped to provide a smoother surface for the growth of a conformal film. The protonic nature of the substrate was not compromised upon this modification.

The highest quality CGO film obtained with the new screen-printed substrate required 12 hours of deposition time with 45 sccm of argon and 5 sccm of oxygen of gas flow at 550°C. One magnetron was used to obtain this sample. In figure 29 a landscape SEM image shows dark spots which most likely indicate the zones of the substrate which remain uncovered by the CGO thin film. Whether this is due to the topology of the substrate or a lack of affinity of the bombarding CGO particles for those areas is unknown.

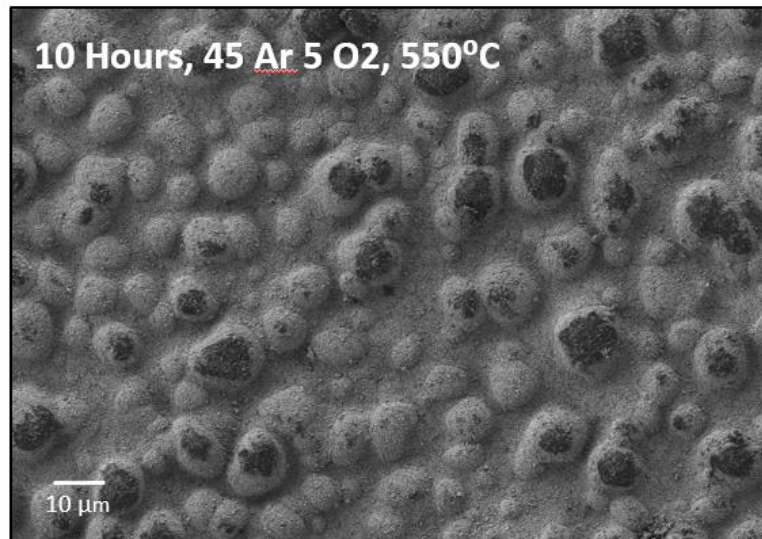


Figure 29: CGO deposited on modified screen printed BCZYYb substrate

Despite issues with total coverage, the film quality in the covered areas is encouraging. Figure 30 presents a continuous and seemingly densified segment of film. However, the grain formation is rather irregular. Upon closer inspection in the image on the right, gaps are observed with diameters in the range of 100 – 200 nanometers in the CGO layer.

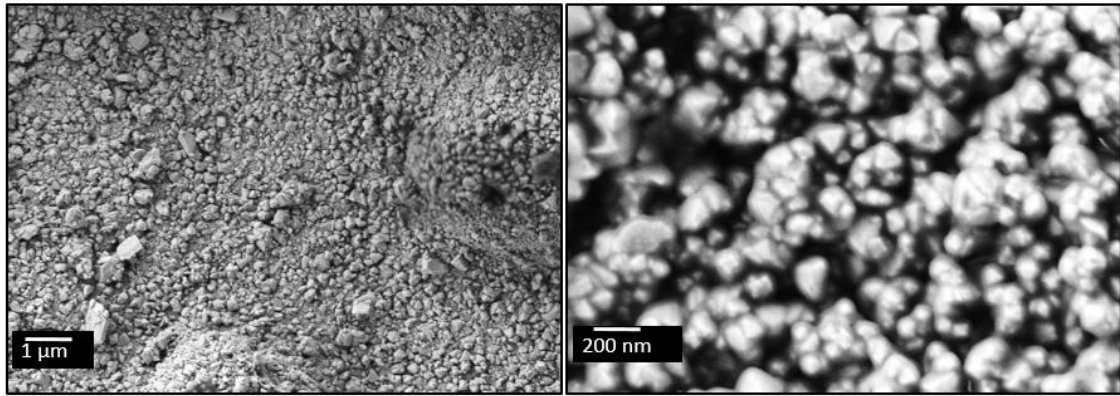


Figure 30: SEM images of CGO deposited on modified BCZYyb substrate

The XRD patterns of the deposited film and the uncovered substrate are shown in figure 31. The presence of the BCZYyb pattern allows for easy observation of the CGO peaks. The CGO film pattern shows the expected fluorite cubic structure (ICDD 00/043/1002). No peaks that correspond to the dopant oxide (Gadolinium Oxide) are present which confirms the full incorporation of the gadolinium into the lattice framework. The peaks are slightly shifted compared to those of a pure cerium oxide sample due to deviations in the cell dimensions caused by the incorporation of the doping particles.

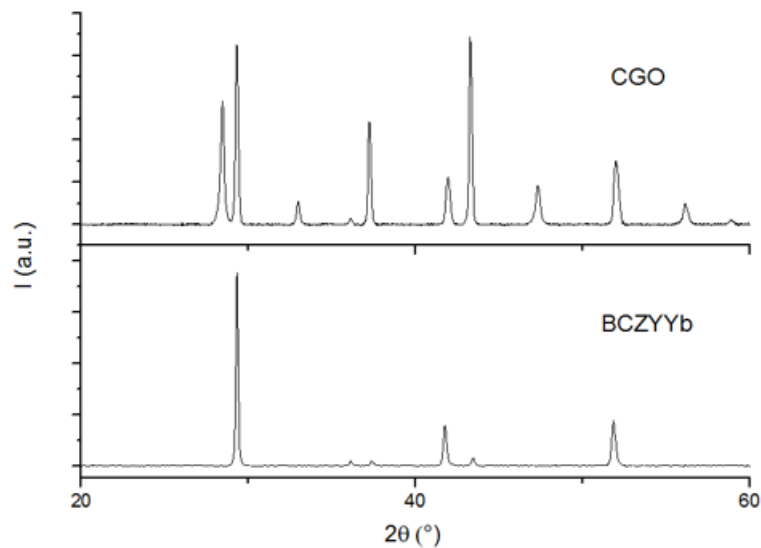


Figure 31: XRD plots of CGO thin film deposited on top of BCZYyb substrate and of pre-deposition BCZYyb substrate

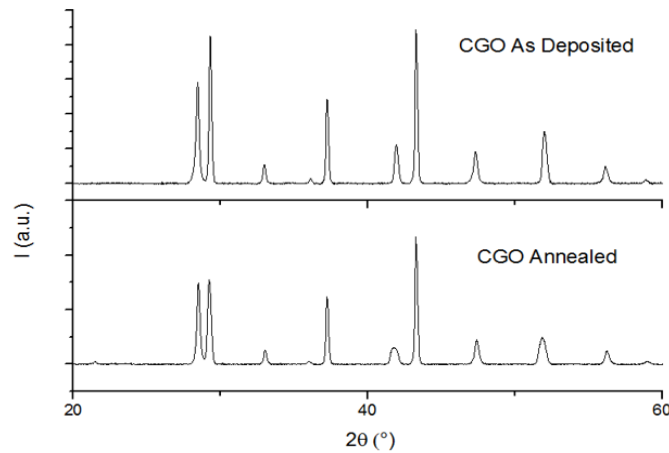


Figure 32: XRD plots of CGO thin film deposited on BCZYyb before and after annealing

To promote grain growth and film densification the CGO sample was annealed in air at 800°C for 2 hours. Research has shown that the cell parameters for lanthanide doped ceria oxide increase linearly with temperature. The XRD patterns of the sample before and after annealing are shown in figure 32. High temperatures are known to increase crystallinity and cause grain growth, these phenomena are confirmed by the narrower more intense peaks in the XRD plot of the annealed sample. The fluorite structure remains after thermal treatment and no phase change is observed. In figure 33, SEM micrographs comparing the annealed and as-deposited samples are presented. The images show that the film has become more homogenous consisting of larger more spherical particles. Nonetheless, as is evident in the images, the film is still porous due to space between the grains and the presence of various pinholes [12].

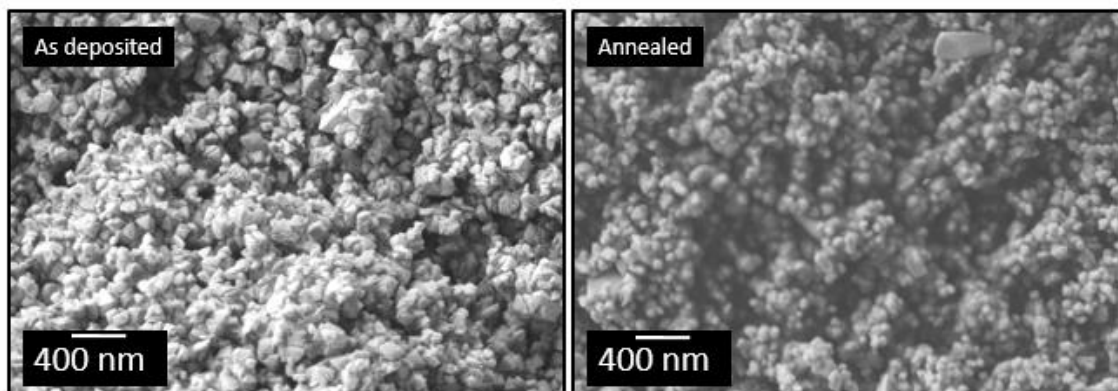


Figure 33: SEM images of CGO thin film on top of BCZYyb substrate before and after annealing

Images of another annealed sample deposited under the same conditions as the samples in figure 33 are shown in figure 34. Once again, the annealed film is comprised of relatively homogeneous particles which are more spherical in nature than those of the as-deposited sample. Based on these images, it is inconclusive whether the porosity has decreased or not. Given the persistence of film porosity and the small change in unit cell parameters according to XRD analysis, it is unsure that annealing under these conditions contributes significantly towards film densification. Due to time restrictions these were the final CGO samples obtained. Significant progress was made towards film conformality, but more experimentation is required to determine how to obtain the desired morphology.

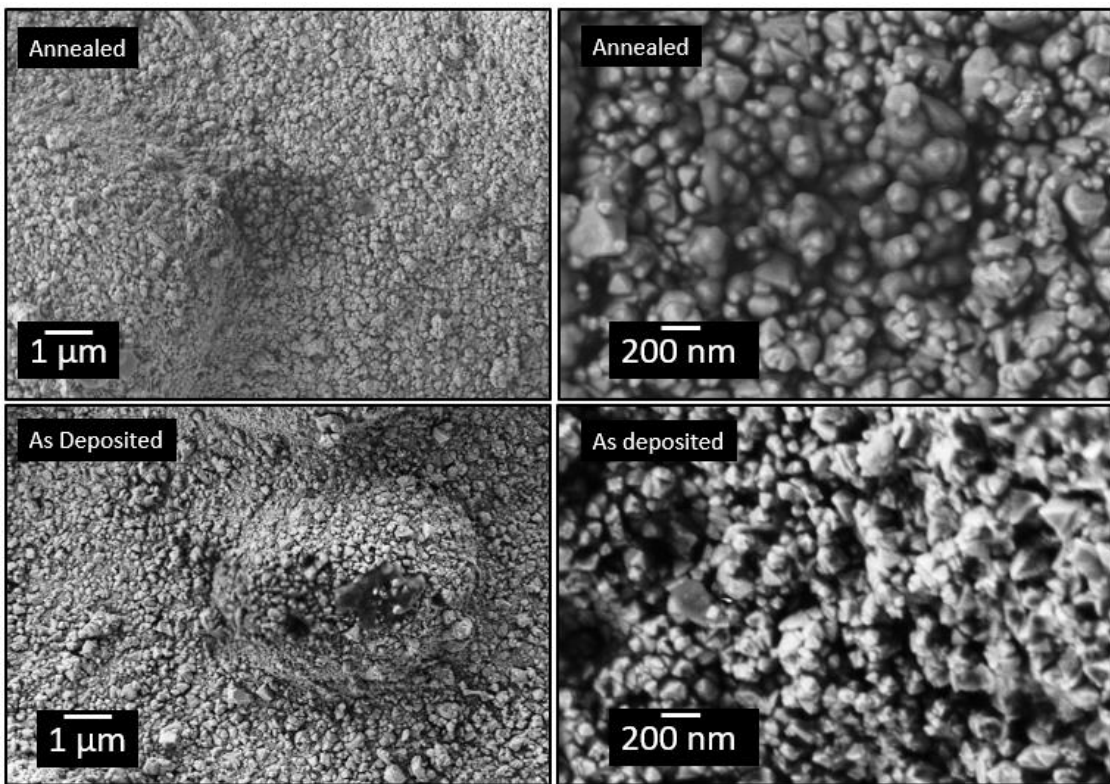


Figure 34: SEM Images of CGO thin film on top of BCZYb substrate before and after annealing

5. Future Action

This project was successful in finding the optimal deposition conditions for conformal thin films of palladium and palladium-copper alloy as well as for the composite GCO/Pd membrane. These metallic membranes possess morphologies, which upon visual inspection, are ready to be employed as selective proton conductors. Due to the time restrictions associated with this thesis, typical membrane characterization tests were not performed. The logical next step in the development of the sputtered membranes would be to carry out an electrochemical characterization via hydrogen permeation testing. A structural characterization of the films is necessary, but permeation testing is required to truly understand the effectiveness of the membrane. Thin film membranes are economically advantageous, and sputtering is a cheap and consistent method for their production. However, before they are applicable in industry their properties must be comprehensively determined. Permeation testing would provide further characterization by quantifying the stability, selectivity and hydrogen flux of the membranes. As a result of this work, a GCO/Pd membrane supported on Anodisc is ready for immediate characterization via permeation. Furthermore, the conditions to create test-ready pure palladium and palladium-copper alloyed membranes have been determined.

Proton and ion conducting membranes working together is a relatively young area of research. The composite membranes have potential applications in complex membrane reactors in which two reactions work together to increase performance. The findings in this thesis are a significant step towards their implementation for such applications. Through manipulation of sputtering variables and substrate modification, the film quality was vastly improved from the initial depositions to the last. However, some further structural investigation into CGO thin films on the BCZYYb proton conductor should be carried out with the aim of determining how to obtain a fully densified and homogenous thin film. To be specific, even longer deposition times and co-sputtering configurations should be tested. As well as different sputtering temperatures and gas flows which may be outside the capacity of the sputtering machine used in this work. Given the success of the substrate modification, more research should be done to see if an even more favorable surface for film growth can be created without compromising its conductive properties. Furthermore, although it seemed that annealing had little impact, longer exposure times and higher temperatures should be explored to confirm that the treatment step is ineffective. Once an acceptable film has been obtained, the next sensible step for further development would be permeation measurements testing both the protonic and ionic conductivity of the membrane.



6. Conclusions

In this master's thesis, a comprehensive characterization was carried out on three types of thin film conductors supported on ceramic membranes prepared via sputtering. Palladium, calcium doped gadolinium oxide and gadolinium doped cerium oxide were characterized structurally using the XRD, EDS and SEM methods. The goal of the structural characterization was to determine which deposition conditions and post-processing treatments should be employed to obtain a dense and homogenous film. In addition, the 4-point DC method was used to attempt to electrochemically characterize the GCO thin films.

In the case of palladium thin films deposited onto porous ceramic substrates, the ideal deposition conditions along with a post-deposition annealing step gave a visually densified thin film. However, upon annealing in hydrogen, the thin film delaminated from the ceramic support. To prevent delamination, various samples were prepared consisting of palladium alloyed with copper and silver. A thin film of palladium co-sputtered with 8YSZ was also prepared. Significant morphological changes were observed upon the incorporation of the new materials into the film. Alloying with just a small percentage of copper (EDX measurements were used to determine composition) produced a dense and rather homogenous film with more cubical grains than those of pure palladium. No annealing was performed on the copper-alloyed film. The silver-alloyed film gave a homogenous film with rounder grains, but many pinholes were present in the film. Upon annealing, the silver-alloyed film also delaminated from the substrate. The ceramic-metal composite film did not delaminate upon annealing but failed to produce a desirable film morphology. Further research should experiment with ways to prevent delamination upon annealing as it was a helpful technique for post-deposition film densification. A method found in literature claims that a polymeric layer between the substrate and thin metallic film increases adhesion. Furthermore, additional alloying compositions should be explored with copper and silver. In this study, very small amounts of the other metals were incorporated into the layer. Films with a higher silver concentration should be prepared to see if they are able to maintain adhesion after annealing. In addition to possibly increasing adhesion, silver and copper can benefit the membrane by alleviating phase transition induced mechanical stresses and lowering costs [23].

The GCO thin film was deposited onto quartz substrates using deposition conditions from a previous work found to produce an acceptable thin film. The samples were then annealed to ensure full crystallinity. XRD plots showed that the thin films adapted the



expected cubic unit cell structure and confirmed the increase in crystallinity upon annealing. The results of the electrochemical characterization of the GCO thin films via the four-point technique proved to be inconclusive. The results were inconsistent with what was expected, and the collected data was often erroneous. The four-point test is still a useful method for qualitatively determining contributing conductivities. Other applied current ranges should be explored, and new samples should be fabricated for conductivity testing. Hydrogen permeation testing of a GCO membrane sandwiched between current collectors is another option for confirming protonic conductivity should the four-point test prove to be impossible with the thin films.

The preliminary GCO-palladium membrane configuration was successfully fabricated via the sputtering deposition of two layers onto the A-tech and Anodisc membranes. Here, a seemingly dense layer of GCO was formed on top of the palladium on the Anodisc substrate. This goal was not achieved for the layered membrane on the A-tech substrate as the SEM images showed a non-homogenous and porous thin film. The increased quality of the Anodisc supported membrane may be attributed to the greater smoothness of the Anodisc surface. Other deposition conditions should be tested to see if it is possible to attain a satisfactory layer on the A-tech substrate. Annealing steps would be of interest as well considering its success in densifying the pure palladium film and improving the crystallinity of the GCO thin film. However, delamination of the composite film from the substrate would still be a possibility. An A-tech supported membrane would be useful due to the substrate's greater sturdiness and higher resistivity to temperature compared to the Anodisc material. Permeation testing must be carried out with the sandwich membranes to confirm its density. In addition, permeation testing would allow for confirmation of the proton conducting nature of the GCO thin film. Since the 4-point conductivity results were inconclusive, permeation testing of these sandwich membranes is even more critical.

In the case of CGO sputtered on BCZYYb, a fully dense film was not obtained. However, a better understanding of how sputtering conditions affect film morphology was achieved and the film quality was substantially increased throughout the work. It was determined that to form a dense ceramic layer on top of an irregular surface like that of BCZYYb, long deposition times are required. More complete coverage was sought by doubling deposition rate via co-sputtering and increasing the time from 1 hour to 5 hours. Visual observations and readings from the power source suggested that the magnetrons were not depositing at the same rate. Thus, subsequent depositions were performed using one magnetron for 10 hours. The morphology of the two films was distinct but neither appeared to be fully dense. The most desirable film was produced



after modifying the substrate by screen printing a thin layer of BCZY on top of the co-doped nickel enriched substrate. The thin layer provided a smoother surface for deposition to promote better film growth. The layers of CGO on the modified substrates were the most promising with areas of full density and a high level of homogeneity. Highly magnified SEM images showed the presence of pinholes and there remained areas of uncovered substrate. Both XRD plots and SEM images showed that annealing the samples at 800°C in air had little effect on the morphology of the CGO layer. Further structural investigation of these membranes is required before electrochemical characterization can be performed.



INSTITUTO DE
TECNOLOGÍA
QUÍMICA



EXCELENCIA
SEVERO
OCHOA

46



CSIC
CONSEJO SUPERIOR DE INVESTIGACIONES CIENTÍFICAS



UNIVERSITAT
POLITÈCNICA
DE VALÈNCIA

7. Bibliography

- [1] S. Yun y S. Ted Oyama, *Correlations in palladium membranes for hydrogen separation: A review*, 2011.
- [2] N. A. Al-Mufachi, N. V. Rees y R. Steinberger-Wilkens, *Hydrogen selective membranes: A review of palladium-based dense metal membranes*, vol. 47, Elsevier Ltd, 2015, pp. 540-551.
- [3] V. Z. Mordkovich, Y. K. Baichtock y M. H. Sosna, «The Large Scale Production of Hydrogen from Gas Mixtures A USE FOR ULTRA THIN PALLADIUM ALLOY MEMBRANES».
- [4] S. Adhikari y S. Fernando, *Hydrogen membrane separation techniques*, vol. 45, 2006, pp. 875-881.
- [5] SONIA ESCOLÁSTICO ROZALÉN, «MEMBRANAS DE SEPARACIÓN DE GASES BASADAS EN CONDUCTORES IÓNICOS MIXTOS Y SUS APLICACIONES EN CATÁLISIS,» 2012.
- [6] D. K. Babi, M. S. Cruz y R. Gani, «Fundamentals of process intensification: A process systems engineering view,» de *Process Intensification in Chemical Engineering: Design Optimization and Control*, Springer International Publishing, 2016, pp. 7-33.
- [7] T. Norby y Y. Larring, «Current Opinion in Solid State Materials Science,» 1997.
- [8] I. Riess, «Mixed ionic-electronic conductors-material properties and applications».
- [9] Gopalan Srikanth, «Using Ceramic Mixed Ionic and Electronic Conductors for Gas Separation,» *Green Manufacturing*, 2002.
- [10] J. Sunarso, S. Baumann, J. M. Serra, W. A. Meulenbergh, S. Liu, Y. S. Lin y J. C. Diniz da Costa, *Mixed ionic-electronic conducting (MIEC) ceramic-based membranes for oxygen separation*, 2008.
- [11] F. Toldrá Reig y J. Manuel Serra Alfaro Valencia, «Development of electrochemical devices for hydrocarbon sensing purposes in car exhaust gases,» 2018.
- [12] M. B. Ramírez, J. Manuel, S. Alfaro, J. Marcial Gozávez y Z. Valencia, «New solid state oxygen and hydrogen conducting materials. Towards their applications as high temperature electrochemical devices and gas separation membranes,» 2013.
- [13] A. Atkinson, «Chemically-induced stresses in gadolinium-doped ceria solid oxide fuel cell electrolytes,» *Solid State Ionics*, 2003.
- [14] T. Norby, «Solid-state protonic conductors: principles, properties, progress and prospects,» 1999.



- [15] T. Norby, O. Dyrлие y P. Kofstad, «Protons in Ca-doped La₂O₃, Nd₂O₃ and LaNdO₃,» *Solid State Ionics*, Vols. %1 de %253-56, nº PART 1, pp. 446-452, 1992.
- [16] Y. Larring, «Protons in rare earth oxides,» *Solid State Ionics*, vol. 77, pp. 147-151, 26 7 2002.
- [17] D. R. Clark, «NANOIONIC PROTON CONDUCTIVITY ENHANCEMENT IN SOLID-STATE REACTIVE».
- [18] G. Bräuer, «Magnetron Sputtering,» de *Comprehensive Materials Processing*, vol. 4, Elsevier Ltd, 2014, pp. 57-73.
- [19] «Zeiss Microscopy,» [En línea]. Available: <https://www.zeiss.com/microscopy/int/products/scanning-electron-microscopes/sigma.html>. [Último acceso: 18 August 2019].
- [20] G. Vijaya, M. Muralidhar Singh, M. S. Krupashankara y R. Kulkarni, «Effect of Argon Gas Flow Rate on the Optical and Mechanical Properties of Sputtered Tungsten Thin Film Coatings,» de *IOP Conference Series: Materials Science and Engineering*, 2016.
- [21] Y. H. Ma, I. P. Mardilovich y E. E. Engwall, «Thin composite palladium and palladium/alloy membranes for hydrogen separation,» de *Annals of the New York Academy of Sciences*, 2003.
- [22] C. Hernandez Londono, L. Combemale, F. Gao, A. Billard y P. Briois, «Properties of Gadolinium-doped Ceria (GDC) Films Deposited by Reactive Magnetron Sputtering Processes,» *ECS Transactions*, vol. 78, nº 1, pp. 1189-1193, 24 7 2017.
- [23] S. Uemiya, T. Matsuda y E. Kikuchi, «Hydrogen permeable palladium-silver alloy membrane supported on porous ceramics,» *Journal of Membrane Science*, vol. 56, nº 3, pp. 315-325, 1991.
- [24] R. Armitage, M. Rubin, T. Richardson, N. O'Brien y Y. Chen, «Solid-state gadolinium-magnesium hydride optical switch,» *Applied Physics Letters*, vol. 75, nº 13, pp. 1863-1865, 27 9 1999.
- [25] A. Cortés Villena, «Desarrollo de electrocatalizadores basados en clústeres de óxido de cobalto para Pilas de Combustible de Membrana de Intercambio Protónico,» 14 1 2019.
- [26] S. Dueñas, H. Castán, H. García, A. Gómez, L. Bailón, K. Kukli, T. Hatanpää, J. Lu, M. Ritala y M. Leskelä, «Electrical Properties of Atomic-Layer-Deposited Thin Gadolinium Oxide High-k Gate Dielectrics,» *Journal of The Electrochemical Society*, vol. 154, nº 10, p. G207, 24 8 2007.
- [27] J. Gerblinger, W. Lohwasser, U. Lampe y H. Meixner, «High temperature oxygen sensor based on sputtered cerium oxide,» *"Sensors and Actuators, B: Chemical"*, 1995.
- [28] V. Jayaraman, Y. S. Lin, M. Pakala y R. Y. Lin, «Fabrication of ultrathin metallic membranes on ceramic supports by sputter deposition,» *Journal of Membrane Science*, 1995.

- [29] Y. Larring y T. Norby, «The equilibrium between water vapour, protons, and oxygen vacancies in rare earth oxides,» *Solid State Ionics*, 2002.
- [30] Y. Lin, S. Fang, D. Su, K. S. Brinkman y F. Chen, «Enhancing grain boundary ionic conductivity in mixed ionic–electronic conductors,» *Nature Communications*, vol. 6, nº 1, p. 6824, 10 11 2015.
- [31] L. L. Pan, G. Y. Li y J. S. Lian, «Structural, optical and electrical properties of cerium and gadolinium doped CdO thin films,» *Applied Surface Science*, 2013.
- [32] D. Pérez-Coll, E. Céspedes, A. J. Dos santos-García, G. C. Mather y C. Prieto, «Electrical properties of nanometric CGO-thin films prepared by electron-beam physical vapour deposition,» *Journal of Materials Chemistry A*, vol. 2, nº 20, p. 7410, 2014.
- [33] S. Ricote, N. Bonanos y G. Caboche, «Water vapour solubility and conductivity study of the proton conductor $\text{BaCe}_{0.9-x}\text{Zr}_x\text{Y}_{0.1}\text{O}_{3-\delta}$,» *Solid State Ionics*, 2009.
- [34] T. Schober, «On the use of Pd filters on proton conducting SOFC ceramics,» *Ionics*, vol. 9, nº 3-4, pp. 297-300, 2003.
- [35] M. Shirpour, G. Gregori, R. Merkle y J. Maier, «On the proton conductivity in pure and gadolinium doped nanocrystalline cerium oxide,» *Phys. Chem. Chem. Phys.*, vol. 13, nº 3, pp. 937-940, 2011.
- [36] M. T. Ta, D. Briand, Y. Guhel, J. Bernard, J. C. Pesant y B. Boudart, «Growth and structural characterization of cerium oxide thin films realized on Si(111) substrates by on-axis r.f. magnetron sputtering,» *Thin Solid Films*, 2008.
- [37] T. Yamaguchi, H. Shimada, U. Honda, H. Kishimoto, T. Ishiyama, K. Hamamoto, H. Sumi, T. Suzuki y Y. Fujishiro, «Development of anode-supported electrochemical cell based on proton-conductive $\text{Ba}(\text{Ce},\text{Zr})\text{O}_3$ electrolyte,» *Solid State Ionics*, 2016.
- [38] S. YUE, F. WEI, Y. WANG, Z. YANG, H. TU y J. DU, «Phase control of magnetron sputtering deposited Gd_2O_3 thin films as high- κ gate dielectrics,» *Journal of Rare Earths*, 2008.



Agradecimientos:

Thank you first to my family for supporting me and allowing me to make this crazy decision to come to Spain for a year and study this Masters. Thank you to Lauren for sticking with me throughout this entire process.

Thank you to Fidel for guiding me, the helpless American who could barely speak Castellano when I arrived. Without him I would still be trying to figure out how to turn on the sputtering machine. He was extremely patient, and I am very grateful for all his help. Thank you also to all the members of the Pilas lab group for helping me figure out things in the lab, teaching me about this amazing country and helping me improve my Spanish at lunch. Thank you also to Jose Serra for letting me be part of this incredible, collaborative and kind group of researchers.

Thank you to all of my master's classmates for being my friends, helping me learn the ropes of how university works in Spain and explaining things in lectures which I did not understand.

Mostly thank you to everyone who was so patient with me when they certainly did not have to be.



INSTITUTO DE
TECNOLOGÍA
QUÍMICA



EXCELENCIA
SEVERO
OCHOA

50



CSIC
CONSEJO SUPERIOR DE INVESTIGACIONES CIENTÍFICAS



UNIVERSITAT
POLITÈCNICA
DE VALÈNCIA